TECHNICAL MEMORANDUMS

NATIONAL ADVISORY COMMITTEE FOR AERONAUTICS

No. 1041

TAIL BUFFETING

By G. Abdrashitov

Central Aero—Hydrodynamical Institute

Washington
February 1943

NATIONAL ADVISORY COMMITTEE FOR AERONAUTICS

TECHNICAL MEMORANDUM NO. 1041

TAIL BUFFETING*

By G. Abdrashitov

An approximate theory of buffeting is here presented, based on the assumption of harmonic disturbing forces. Two cases of buffeting are considered: namely, for a tail angle of attack greater and less than the stalling angle, respectively. On the basis of the tests conducted and the results of foreign investigators, a general analysis is given of the nature of the forced vibrations, the possible load limits on the tail, and the methods of elimination of buffeting.

INTRODUCTION

The term "buffeting" in its broad sense is applied to the forced vibrations of any parts of the airplane under the aerodynamic action of the wake in which such parts are situated, though in general aeronautic practice the term is restricted to this type of vibration of the tail surfaces under the action of the disturbing wake of the wing, the phenomenon occurring under certain flight conditions. Depending on the values of the parameters that characterize the wake, the tail is subjected to additional dynamic loads of various kinds which may lead to its failure or otherwise render normal operation of the airplane difficult.

The buffeting problem first took on a serious aspect after the well-known accident of the Junkers airplane at Meopham. The unusual circumstances of the accident led scientific organizations in England and Germany to undertake detailed investigations as to the possible causes that may have brought it about. The English conducted extensive laboratory investigations and arrived at the conclusion that the most probable cause of the accident was buffeting of the tail. In these investigations on schematized models of the airplane it was accurately established that at large angles of attack of the wing the

*Report No. 395, of the Central Aero-Hydrodynamical Institute, Moscow, 1939.

tail situated in the aerodynamic wake of the wing vibrates intensely, the amplitude of the vibration increasing with increase in the velocity.

A detailed investigation of the place of the accident showed the presence of large rising air currents and the following explanation was therefore given of the causes of the accident: The airplane, flying horizontally with great velocity, suddenly entered a region of strong rising gusts as a result of which there was a sharp increase in the angle of attack with the formation of flow separation at the wing. The tail located in the wake was subjected to intense forced vibrations which thus brought about the accident.

To the investigation of this accident were also devoted the papers of a group of German investigators under the leadership of Blenk (reference 1). The latter conducted laboratory and flight investigations and also detailed dynamic investigations of the same type of airplane in the hangar. The laboratory investigations showed that it was entirely possible for the airplane to enter the buffeting state; but in actual flight, except during a steep glide, buffeting of the tail was not observed even once. For this reason, after analyzing all investigations, Blenk arrived at the conclusion that the accident of the JU 13 could not have been due to buffeting.

The importance of the investigations of Blenk lie in the test procedure which he consistently employed. He was the first to apply the moving picture camera to investigate buffeting on the airplane in flight. A high-speed camera was mounted in the pilot's cabin and enabled the simultaneous recording of the motion of the tail surface tip and of a silk string placed ahead of it. Figure 1 shows a part of the film, taken during a steep glide on the wing when the tail begins to buffet. On carefully studying the photographic record, a relation may be established between the fluctuation of the tail surface and the silk string. The fundamental conclusions from these tests of Blenk are the following:

1. The tail surfaces at large angles of attack of the wing enter a region of vortices springing from the intersection of the wing and fuselage, and in all these cases vibration of the tail is observed; the vortices arise at both sides of the fuselage and usually in an unsymmetric manner. The vibrations of the tail are of an irregular

character but large amplitudes, as a rule, are rare and continue only for a very short time.

2. Regular periodic vibrations of the tail surfaces are also entirely possible. For this reason, the possibility of entry into a resonance condition constitutes a real danger.

3. The amplitudes increase very slowly with the velocity and do not attain their maximum values at any definite velocities.

As will be shown in what follows, not all results obtained on the Junkers airplane tests may be generalized and accepted without any reservations, assuming all conclusions as irrefutably proven. Even so, the work of Blenk is the most thorough in this field of investigation.

In 1933 two papers devoted to buffeting investigation appeared by Duncan (references 2 and 3). This author studied the vibrations of an elastically hinged "detector" having the form of a stiff airfoil attached at its root to a streamline base piece. It should be said that such a scheme, suitable for the determination of the frequency, cannot give the corresponding amplitude of the acting forces, and this is one of the chief defects of this method. Moreover, the detector cannot vary its angle of attack.

In 1934 Hood (reference 3) carried out wind tunnel investigations on the elimination of buffeting observed in flight of a given airplane. Similar flight investigations were conducted by Biechteler (reference 4) in Germany. This completes essentially the fundamental literature on buffeting.

In the routine testing of airplanes the buffeting problem is sometimes practically encountered. At the present time a large number of very simple devices are already available for the elimination of buffeting. It should be pointed out, however, that these devices are based only on a qualitative estimate of the phenomenon, and the quantitative problems involved are not even approximately solved. The difficulty of the problem lies in the fact that the actual nature of the aerodynamic wake behind bodies and the laws of the dynamic processes that may occur in the wake have not yet been established. From this fact follows also the impossibility of an exact determination of the magnitude of the forces required for making the tail undergo

forced vibrations. The questions of the viscosity of the fluid and the nonstationary character of its motion, which factors in the usual applied aerodynamics of the airplane may often be neglected, here assume predominating importance.

The complete solution of the buffeting problem thus embraces, as yet, unsolved aerodynamic problems. For this reason, it is necessary to seek indirect methods which, while not encompassing the problem in its entirety, make it possible to determine states which are critical as regards accidents. The present paper is devoted to an exposition of these critical cases.

NOTATION

V flow velocity

P lift force

t tail chord

τ time

α_t angle of attack of tail

α_w angle of attack of wing

α_{tc} critical (stalling) angle of attack of tail surface

α_{wc} critical (stalling) angle of attack of wing

$\frac{\partial C_y}{\partial \alpha}$ derivative of lift coefficient with respect to angle of attack

$\frac{\partial C_{mE}}{\partial \alpha}$ derivative of moment of aerodynamic forces about the elasticity axis of the tail with respect to the angle of attack

ω angular frequency of the disturbance forces

ν number of vibrations per second

l half span of tail

EI stiffness of tail in bending

GI_p stiffness of tail in torsion

m unit mass of tail

x_o distance of center of gravity from nose of profile

σ distance of center of gravity from elasticity axis at section considered

I_m unit moment of inertia of tail surface with respect to its stiffness axis

ρ density

y deflection of tail surface at given cross section

θ angle of torsion at given section

The x-axis is taken along the tail span and the y-axis at right angles to it.

I. SOME DATA ON THE WAKE BEHIND A BODY

A large number of papers have dealt with the problem of what occurs in the flow behind a body. It is, however, impossible at the present time to point to even a single paper which might throw light on the problem of the wake from the point of view of every-day practical needs. All of these papers concern themselves mainly with regions of very small Reynolds number; and at times, restrict themselves to results of purely visual observations.

The behavior of light particles moving in the flow about a body shows that there is no absolutely dead region behind the body but that a complicated process of fluid motion occurs. All bodies placed in such a wake are subject to vibrational motions. From the point of view of the well-known Karman theory, this may be explained by the periodic shedding of discrete vortices from the body, thereby producing the same type of velocity field and also field of force behind the body. In general, the buffeting theory may be set up both on the basis of pure wave motion of the fluid behind the body and on the basis of the vortex wakes of Karman, both assumptions leading to the same results. In the first case, it is necessary to know the amplitude and frequency of the wave and in the second, the frequency and circulation of the individual vortices. For this

reason, without restricting ourselves to any definite scheme, we shall consider that behind the bodies a vibration process takes place for which two fundamental parameters must be known; namely, the amplitude and frequency.

The problem of the wave amplitudes or of the circulation of the separating vortices is as yet unsolved. With regard to the frequency, a criterion has already been established connecting the frequency of vibration with the velocity. This is the Strouhal number (reference 5) given by

$$S_t = \frac{\nu b}{V}$$

where

ν is the number of vibrations per second

b a linear dimension (for example the chord)

V the flow velocity

A large number of investigations are concerned with the determination of the Strouhal number. There may be mentioned, for example, the papers by Strouhal, Blenk, Fage, Duncan, and others. The problem is to determine the vibration frequency as a function of the velocity. Fundamentally, three methods are employed for this purpose: The first is the acoustic method by which the intensity or pitch of the sound of thin streamlined wires in the stream is measured, since it has been found that the vibration of the wires is due to the periodic shedding of vortices from it. This method was employed by Strouhal and later by Blenk. A difficulty should here be pointed out which unavoidably leads to an error in the results; namely, the requirement of very thin wires. The method requires using very thin wires in streams of very high velocity and separating from the general sound produced that sound emitted by the wire - considerations which lead to a very complicated setup including various sound analyzers. The test, moreover, often becomes very complicated if any external body emits a sound of the same type as the wire. The second is the thermal method, using the well-known hot wire anemometer; this method being the one widely employed in English and American investigations. In the flow behind the body is placed a very thin heated wire which, under the action of the variable flow velocities, changes its electrical properties, from which the frequency of vibration can be determined. Finally, the third method is

that of measuring the frequency of the vibrations from the behavior of various bodies placed in the stream - silk streamers, vanes, and so forth. By these methods, fundamentally, were obtained the data on the Strouhal numbers for various bodies. We shall present some results obtained by different authors.

Plate

Fage (reference 6) investigated in detail the flow behind a plate and obtained the results given in the table below:

Strouhal Number at Various Angles of Attack for Flat Plate and Airfoil

α	Plate	Airfoil
90	0.146	0.15
60	.15	.154
50	.15	.15
45	.145	.148
40	.148	.157
30	.153	.15
20	.164	.152

The measurements were made by the method of the hot-wire anemometer. The mean value of the Strouhal number of the plate is equal to 0.148 for a range of angle of attack of 30° to 90°. Blenk (reference 7) gives for the plate $S_t = 0.18$ where

$$St = \frac{b\,\nu}{V} \cdot \sin \alpha$$

Cylinder

In the case of the cylinder the results of acoustic measurements only are available in the literature, with the single exception of the work of Relf (reference 8), where the results from different methods of measurement are combined and a curve of S_t against Re is obtained (fig. 2). According to the results of Relf, for the

cylinder $S_t = 0.18$; but according to Blenk $S_t = 0.207$. Strouhal gives, for the cylinder, a value which agrees with that of Blenk.

Some further remarks should be made with regard to the Relf curve (curve II, fig. 2). The numerical values are not of special interest because they include only the two extreme points of the curve and at the stalling portion, two or three measurements that disagree with each other are given. A comparison, however, with the drag curve (curve I) confirms the well-known fact in aerodynamics that the frequency of the vibration is associated with the width of the wake and the latter, as is known, depends in turn on the position of the point of separation of the flow at the cylinder. The point of separation at Re_{crit} recedes sharply and narrows the wake and therefore sharply increases the frequency of the vibration so that if the narrowing of the wake is not taken into account and everything is referred to the diameter, it is possible at Re_{crit} to obtain a discontinuity of the Strouhal number as shown on the Relf curve.

Airfoil

The papers of Fage, Blenk, Duncan, and others are concerned with the investigation of the Strouhal number behind airfoil sections. The Reynolds number in these papers does not exceed a value of the order of 200,000. The results of Fage, after recomputation with reference to the projection of the chord on the plane perpendicular to the flow, give a value $S_t = 0.15$ for $\alpha_w = 24^\circ - 90^\circ$. These results are shown in the table above.

The same results are obtained by Duncan from his measurements with a detector. The investigations of Blenk gave for wing profiles the value $S_t = 0.21$.

Summarizing all the above results, the following conclusion may therefore be arrived at: The results of direct measurements of the vibrations of the flow give a Strouhal number for the plate and airfoil equal approximately 0.148 to 0.150. From acoustic measurements for the cylinder $S_t = 0.207$, for the plate $S_t = 0.18$ and for the airfoil $S_t = 0.21$. From these measurements one important conclusion is derived; namely, that the value of the Strouhal number, taken over the middle range of resistance,

practically has the same value for all bodies. This very important fact greatly facilitates both the investigation of the fundamental characteristics of buffeting and its practical elimination. The extent to which these two groups of values of S_t correspond to actuality will be considered in detail in what follows.

The region of propagation of the disturbed wake is no less important for the problem of buffeting. The problems associated with the wake have been extensively treated in the literature. The fundamental method employed in obtaining the results is that of measuring the total head with a pitot tube, a boundary point of the wake being considered a point at which the dynamic pressure no longer varies along the normal to the direction of the velocity.

The curves of figure 3, taken from the paper by Petersohn (reference 9), show that the downwash angle behind the wing increases up to $\alpha_{w\ cr}$ and then with increasing angle of attack begins to decrease rapidly and at a certain definite angle of attack entirely vanishes. This, as will be shown below, is of great importance in the problem of buffeting.

Although the width of the wake as obtained from the dynamic pressure measurements is satisfactory, to some extent, for a number of problems arising in practice, this is far from the case as regards the problem of buffeting. The curves given in the paper of Duncan (fig. 4) show that the tail vibrates strongly beyond the wake limits obtained with the usual pitot tube. The dotted curves in the figure show the wake boundary behind the body obtained with the pitot tube and the continuous lines are those of equal buffeting intensity, that is, the lines for which the amplitude of tail vibration has the same value. If, for example, over the entire line 1, the value of the amplitude is taken equal to unity; then at line 2 it has a value by only 30 percent less than on the first. In general, on an actual airplane the tail will always be, at angles of attack of the wing above the stall, in the region of influence of the vortices shed from the wing.

II. ACTION OF THE WAKE ON THE TAIL

We assume that in the wake behind the wing is situated a second airfoil. The question arises how an airfoil so

situated will behave, what loads it will experience, and what motions it will execute under these loads. The answer to these questions is fundamental in the theory of buffeting. It follows immediately from the assumed vibratory character of the wake that at each point of the region behind the wing the velocity, variable with respect to time, gives rise to vertical velocity components ahead of a tail set at variable angles of incidence. The latter give rise, naturally, to variable forces and vibrational motion of the tail. To solve the problem of buffeting, it is therefore necessary to know the fundamental parameters of these forces, that is, the frequency and amplitude. The problem of unsteady motion of a wing in a disturbed flow appears so complicated that an attempt to solve it in its general form holds forth little promise at the present time. It is therefore necessary to make a number of assumptions by which the problem may be schematized without impairing its practicality. We shall assume that the stationary condition holds also for the case of buffeting; that is, we shall consider that the general motion of the tail relative to the flow may be subdivided into a large number of time intervals within which the motion may be considered as steady. Otherwise expressed, at each instant of time the aerodynamic forces are determined by the Joukowsky theorem. This is equivalent to the assumption that the lift curve of the airfoil will remain the same as for steady motion. From the assumed nature of the disturbing forces, it follows directly that their maximum possible value is determined chiefly, not by the wake itself but by the wing subjected to it. It is known that the lift on the wing may be increased only up to a certain limiting value $C_{y\ max}$ characteristic of the given wing section. That is to say, an additional angle of attack arising from the vibrational character of the wake may increase or decrease the lift of the tail surface depending on whether or not the total angle of attack exceeds the angle $\alpha_{w\ cr}$. By taking for the amplitude of the force the value corresponding to $C_{y\ max}$ we include the most dangerous condition, the elimination of which automatically assures safety in all the other cases. We shall therefore assume that under forced vibrations, the value of $C_{y\ max}$ of the tail remains constant. This assumption is a direct consequence of the assumption of the stationary condition of the flow. It follows that the character of the motion will vary greatly, depending on whether the tail operates below or above the stall region of the lift curve. In the latter case, as will be shown below, the vibrations will be unstable.

We shall take a very simple example - the case of purely bending vibrations. From the theory of flutter it is known that such type of vibrations will always be damped, the wing itself acting to damp the motion. The case is otherwise if the wing vibrates in the range of the lift curve above the stall. Consider the schematized lift curve (fig. 5). Let the tail surface move from any position A to the position B with any velocity. The relative velocity of the air will then be opposite to the direction of motion of the tail surface. The resultant flow velocity formed of the sum of the horizontal and above-mentioned relative vertical velocity will then form a smaller angle with the tail surface than before, that is, if the tail initially was at an angle of attack α_2 then in the course of its motion to the position B the angle of attack is decreased to the value α_1. But in this case, as is seen from the curve, the lift force increases, that is, is directed along the motion of the tail. The same result is obtained for the motion of the tail to position C. Thus the tail surface, operating in this range of the lift curve, becomes unstable and hence the amplitude of the forces is of importance for the buffeting problem only in the range below the stall, since in the range above the stall the vibrations will diverge independent of the magnitude of the forces. It can be readily shown that the danger of this type of buffeting for the airplane is real. It is known that the downwash angle of the flow above the stall decreases with increase in the angle of attack of the wing and at a certain angle of attack entirely vanishes. The disturbing wake, traveling in the direction of flight, immediately brings the tail surface beyond the stall because $\alpha_{t\ cr}$ is somewhat lower than $\alpha_{w\ cr}$.

We shall consider the simple case of the disturbing forces acting according to the harmonic law. It should be noted that the case of periodic disturbance forces is the most dangerous of all possible cases, since such forces may give rise to any amplitude of vibration and bring the tail into a resonance condition. From this point of view, it seems proper to start our consideration of buffeting with the case of harmonically acting forces as the simplest of periodic forces. We, therefore, shall set

$$\Delta\alpha = A \sin \omega\tau$$

where $\Delta\alpha$ is the increment in the angle of attack produced by the wake ahead of the tail; and A its amplitude.

Then

$$\Delta P = \frac{\Delta C_y}{\Delta \alpha} A \sin \omega\tau \, \rho \, t \, V^2 \, dx$$

or

$$dP = \frac{\partial C_y}{\partial \alpha} A \sin \omega\tau \, \rho \, V^2 \, t(x) \, dx \qquad (1)$$

With the above assumptions, the equation of motion can be very simply set up. It is clear that the equation will be linear nonhomogeneous, its left side being similar to the left side of the equation of wing flutter (reference 10) and on the right side will appear the distributed load due to the disturbing forces. On this basis we shall consider a few examples of possible cases of buffeting when the tail operates below the stall.

Case of Purely Bending Vibrations

The equation of motion is of the form

$$\frac{\partial^2}{\partial x^2}\left(EI \frac{\partial^2 y}{\partial x^2}\right) + m(x) \frac{\partial^2 y}{\partial \tau^2} + \frac{\partial C_y}{\partial \alpha} \rho V t(x) \frac{\partial y}{\partial \tau} = A\rho \frac{\partial C_y}{\partial \alpha} t(x) V^2 \sin \omega\tau \qquad (2)$$

This is the usual equation of the forced vibrations of a beam of variable cross section with loads uniformly distributed along the span.

Let $EI = \text{const}_1$, $m(x) = \text{const}_2$, $t(x) = \text{const}_3$ and set

$$a_1 = \frac{\partial C_y}{\partial \alpha} \rho t; \quad k_1 = A\rho \frac{\partial C_y}{\partial \alpha} t$$

The equation will then assume the simple form

$$EI \frac{\partial^4 y}{\partial x^4} + m \frac{\partial^2 y}{\partial \tau^2} + a_1 V \frac{\partial y}{\partial \tau} = k_1 V^2 \sin \omega\tau \qquad (3)$$

The integration of the nonhomogeneous and homogeneous equations meets with the same difficulty; namely, the determination of the functions $f_n(x)$ of the problem by which the solution of the nonhomogeneous and homogeneous

problems is developed in a series of the form

$$y = \sum_{n=1}^{\infty} f_n(x)\xi_n(\tau) \tag{4}$$

where $f(x)$ are the functions characterizing the form of the vibration of the tail surface and $\xi(\tau)$ gives the change in deflection with time. This is the usual method of Poisson for solving a linear partial differential equation by assuming a solution in the form of the product of two functions, each of which is a function of only one variable; namely, the time and the position on the beam.

We shall rewrite equation (3) in the form

$$EIy^{IV} + m\ddot{y} + a_1 V\dot{y} = k_1 V^2 \sin \omega\tau \tag{3'}$$

where

$$y^{IV} = \frac{\partial^4 y}{\partial x^4}; \qquad \ddot{y} = \frac{\partial^2 y}{\partial \tau^2}; \qquad \dot{y} = \frac{\partial y}{\partial \tau}$$

Its general solution is of the form: $y = y_1 + y_2$ where y_1 is the solution of equation (3'), with the right-hand side set equal to zero and y_2 the particular solution satisfying the equation.

Let

$$y_1 = f(x)\ \xi(\tau)$$

Then, as is known, the homogeneous equation corresponding to equation (3') breaks up into two equations of the form

$$y^{IV} - k^4 f = 0$$

and

$$\ddot{\xi} + \frac{a_1 V}{m}\dot{\xi}^1 + \lambda^2 \xi = 0$$

where

$$k^4 = \lambda^2 \frac{m}{EI}$$

The integral of the first of these equations is

$$f(x) = A_1 \cos kx + B_1 \sin kx + C_1 \cosh kx + D_1 \sinh kx \tag{5}$$

and of the second

$$\xi(\tau) = e^{-x_1 \tau} (A_0 \cos p\tau + B_0 \sin p\tau) \tag{6}$$

where $\chi_1 = \frac{1}{2m} \frac{\partial C_y}{\partial \alpha} \rho V t$; and p is the natural frequency of the tail. It is seen that for positive values of $\frac{\partial C_y}{\partial \alpha}$ the free vibrations are damped and for negative values - that is, for $\alpha_t > \alpha_{t\ cr}$ they are not damped.

The coefficients of expression (5) are determined from the boundary conditions which they must satisfy: namely,

$$\left.\begin{aligned} &\text{for } x = 0, && y = \frac{\partial y}{\partial x} = 0 \\ &x = l, && \frac{\partial^2 y}{\partial x^2} = \frac{\partial^3 y}{\partial x^3} = 0 \end{aligned}\right\} \tag{7}$$

leading to a transcendental equation of the form

$$\cos kl \cosh kl = -1 \tag{8}$$

from which are obtained the following values of kl characterizing the frequencies of vibration of the beam:

$k_1 l$	$k_2 l$	$k_3 l$	$k_4 l$
1.875	4.694	7.885	10.96

It is necessary to point out one assumption which was made in the above discussion; namely, that the modulus of the velocity was equal to the velocity at infinity V. The error involved is of the order of the square of a small value ($\Delta^2\alpha$). This assumption will also apply in what follows.

The particular solution of the nonhomogeneous equation is sought in the form

$$y_2 = \zeta(\tau)\, f(x) \tag{9}$$

We set

$$a_2 = \frac{m}{EI}; \quad c = \frac{a_1 V}{EI} = \frac{\frac{\partial c_y}{\partial \alpha} \rho t V}{EI}; \quad k_o = \frac{k_1}{EI}$$

Equation (3') then becomes

$$f^{IV}\zeta + a_2 f(x)\ddot{\zeta} + cf\dot{\zeta} = k_o V^2 \sin \omega\tau = p_o(x,\tau) \tag{10}$$

The right-hand side, in general, is also a function of the time and of the coordinate of the beam axis and, as is known from the general theory, it may be assumed in the form of a product

$$p_o(x,\tau) = f(x)\, H(\tau) \tag{11}$$

Substituting the above equation in (10) and dividing by f(x), we obtain

$$a_2\ddot{\zeta} + c\dot{\zeta} + k^4\zeta = H(\tau) = \text{const} \sin \omega\tau \tag{12}$$

where the equation $f^{IV} - k^4 f = 0$ was made use of for determining F^{IV}.

Setting

$$\zeta = A \cos \omega\tau + B \sin \omega\tau \tag{13}$$

we obtain

$$\dot{\zeta} = -A\omega \sin \omega\tau + B\omega \cos \omega\tau; \quad \ddot{\zeta} = -A\omega^2 \cos \omega\tau - B\omega^2 \sin \omega\tau$$

Substituting (13) in (12) and equating the coefficients of the sine and cosine terms, we obtain the system

$$\left.\begin{aligned} -a_1 A \omega^2 + cB\omega + k^4 A = 0 \\ -B a_2 \omega^2 - cA\omega + k^4 B = \text{const} = h \end{aligned}\right\} \tag{14}$$

or

$$A(k^4 - a_2\omega^2) + Bc\omega = 0, \quad -Ac\omega + B(k^4 - a_2\omega^2) = h$$

whence

$$A = \frac{hc\omega}{(k^4 - a_2\omega^2)^2 + c^2\omega^2}; \quad B = \frac{h(k^4 - a_2\omega^2)}{(k^4 - a_2\omega^2)^2 + c^2\omega^2}$$

We assume

$$A = U \sin \delta, \qquad B = U \cos \delta$$

It is then readily seen that

$$U = \sqrt{A^2 + B^2} = \frac{h}{\sqrt{(k^4 - a_2 \omega^2)^2 + c^2 \omega^2}} \tag{15}$$

whence

$$y_2 = f(x)\, U \sin(\omega\tau + \delta) = \frac{f(x)h}{\sqrt{(k^4 - a_2\omega^2)^2 + c^2\omega^2}} \sin(\omega\tau + \delta) \tag{16}$$

The maximum deflection of the tail will occur for

$$k^4 = a_2 \omega^2$$

We shall then have

$$y_{2\ max} = \frac{f(x)\ h}{\sqrt{c^2\omega^2}} = \frac{f(x)\ h}{c\omega} \tag{17}$$

Remembering that

$$\omega = \sqrt{\frac{k^4}{a_2}} = \frac{k^2}{\sqrt{a_2}}$$

we obtain

$$y_{2\ max} = \frac{f(x)\ h}{c\frac{k^4}{\sqrt{a_2}}} = \frac{(fx)\ h}{ck^2\ \sqrt{\frac{EI}{m}}} \tag{18}$$

Since $h = \text{const}_1\ V^2$; $\quad c = \text{const}_2\ V$;

we shall have

$$y_{2\ max} = \text{const}\ f(x)\ \frac{V}{\sqrt{\frac{EI}{m}}} \tag{19}$$

that is, the value of the deflections in the case of resonance is determined not only by the elastic properties of the tail but also by the velocity of the flow. For this reason, it is not possible, in general, to speak of

the danger of resonance in buffeting without specifying the velocity at which this resonance occurs.

The same result may be arrived at much more simply by applying the method of Galerkin to the solution of equation (3). We shall first make two reservations which follow immediately from the nature of the problem and which very much simplify it. In the first place, we are not required to find the complete integral of the equation of motion for the simple reason that the buffeting occurs at below-critical velocities for which reason the free vibrations will be damped and will therefore not directly concern us. We shall, therefore, seek only the forced vibrations of a frequency equal to that of the acting forces. In the second place, we shall not concern ourselves with the investigations of the tail vibrations of the higher harmonics, this case being of no practical interest since it is then necessary to take into account the formation of nodes. It is known that the frequency of the vortices of actual airplanes lies within the range of natural frequencies of the tail surface and for this reason the attainment of flow frequencies equal to the higher harmonics of the tail surface would require increasing the velocity almost three times, which in the given case is practically impossible. We shall, therefore, consider the form of the forced vibrations as coinciding with the form of vibration of the fundamental frequency. The equation of vibration of the tail with variable cross section and rigidity for the case of purely flexural vibrations is

$$\frac{\partial^2}{\partial x^2}\left(EI\,\frac{\partial^2 y}{\partial x^2}\right) + m(x)\frac{\partial^2 y}{\partial \tau^2} + \frac{\partial C_y}{\partial \alpha}\,\rho V t(x)\frac{\partial y}{\partial \tau} = A\frac{\partial C_y}{\partial \alpha}\,\rho V^2 t(x)\,\sin\omega\tau \qquad (3')$$

Assuming that the functions $y(x)$ are already known, we seek, according to the general theory, a solution in the form of the product

$$y = f(x)\,\xi(\tau)$$

Substituting in equation (3') and applying the method of Galerkin, we multiply both sides of the equation by $f(x)dx$, integrate over the entire half-span, and obtain

$$\xi(\tau)\int_0^l \frac{d^2}{dx^2}\left(EI\frac{d^2 f}{dx^2}\right) f(x)dx + \ddot{\xi}\int_0^l m(x)\,f^2(x)dx + \dot{\xi}\,\frac{\partial C_y}{\partial \alpha}\,\rho V\int_0^l t(x)\,f^2(x)dx = A\frac{\partial C_y}{\partial \alpha}\,\rho V^2\int_0^l t(x)f(x)dx \qquad (20)$$

It is readily shown from the boundary conditions which f(x) must satisfy that

$$\int_0^l \frac{d^2}{dx^2}\left(EI\frac{d^2f(x)}{dx^2}\right)f(x)\,dx = \int_0^l EI\left(\frac{d^2f}{dx^2}\right)^2 dx.$$

Integrating by parts the integral on the left-hand side

$$\int_0^l \frac{d^2}{dx^2}\left(EI\frac{d^2f}{dx^2}\right)f(x)\,dx = \frac{d}{dx}\left(EI\frac{d^2f}{dx^2}\right)f(x)\Bigg|_0^l - \int_0^l \frac{d}{dx}\left(EI\frac{d^2f}{dx^2}\right)\frac{df}{dx}\,dx.$$

The first term, on account of the boundary conditions, is equal to zero. Integrating the second again by parts, we obtain

$$-\int_0^l \frac{d}{dx}\left(EI\frac{d^2f}{dx^2}\right)\frac{df}{dx}\,dx = -EI\,\frac{d^2f}{dx^2}\frac{df}{dx}\Bigg|_0^l + \int_0^l EI\frac{d^2f}{dx^2}\frac{d^2f}{dx^2}dx = \int_0^l EI\left(\frac{d^2f}{dx^2}\right)^2 dx.$$

Setting

$$\int_0^l EI\left(\frac{d^2f}{dx^2}\right)^2 dx = a; \qquad \int_0^l m(x)f^2(x)\,dx = b;$$

$$\frac{\partial C_y}{\partial \alpha}\rho\int_0^l t(x)f^2(x)\,dx = c, \qquad A\frac{\partial C_y}{\partial \alpha}\rho V^2\int_0^l t(x)f(x)\,dx = d.$$

equation (20) assumes the form

$$a\ddot{\xi}(\tau) + b\ddot{\xi} + c\dot{\xi} = d\sin\omega\tau;$$

$$\ddot{\xi} + \frac{c}{b}\dot{\xi} + \frac{a}{b}\xi = \frac{d}{b}\sin\omega\tau. \tag{20'}$$

Assuming

$$\xi = \bar{A}\cos\omega\tau + \bar{B}\sin\omega\tau,$$

we obtain

$$-\bar{A}\omega^2\cos\omega\tau - \bar{B}\omega^2\sin\omega\tau - \frac{c}{b}\bar{A}\omega\sin\omega\tau +$$

$$+\frac{c}{b}\bar{B}\omega\cos\omega\tau + \frac{a}{b}\bar{A}\cos\omega\tau + \frac{a}{b}\bar{B}\sin\omega\tau = \frac{d}{b}\sin\omega\tau.$$

Equating the coefficients of the cosine and sine terms, we find

$$\bar{A}\left(\frac{a}{b}-\omega^2\right) + \frac{c}{b}\bar{B}\omega = 0; \quad -\bar{A}\frac{c}{b}\omega + \bar{B}\left(\frac{a}{b}-\omega^2\right) = \frac{d}{b}. \tag{21}$$

whence

$$\bar{A} = \frac{\frac{d}{b}\frac{c}{b}\omega}{\left(\frac{a}{b}-\omega^2\right)^2 + \left(\frac{c}{b}\omega\right)^2}; \qquad \bar{B} = -\frac{\left(\frac{a}{b}-\omega^2\right)\frac{d}{b}}{\left(\frac{a}{b}-\omega^2\right)^2 + \left(\frac{c}{b}\omega\right)^2}$$

Setting $\bar{A} = U \cdot \sin\delta; \qquad \bar{B} = U\cos\delta,$

where $U = \sqrt{\bar{A}^2 + \bar{B}^2}; \qquad \operatorname{tg}\delta = \frac{\bar{A}}{\bar{B}},$

we obtain $$y = f(x) \cdot U \cdot \sin(\omega\tau + \delta). \tag{22}$$

where δ is the phase angle

$$y = \frac{f(x) \cdot A \frac{\partial C_y}{\partial \alpha} \rho V^2 \int_0^l t(x) f(x)\, dx \sin(\omega\tau + \delta)}{\int_0^l m(x) f^2(x) dx \sqrt{\left(\frac{\int_0^l EI\left(\frac{d^2f}{dx^2}\right)^2 dx}{\int_0^l m(x) f^2\, dx} - \omega^2\right)^2 + \left(\frac{\frac{\partial C_y}{\partial \alpha}\rho V \int_0^l t(x) f^2\, dx}{\int_0^l m(x) f^2\, dx}\omega\right)^2}}, \tag{23}$$

where the expression

$$\frac{\int_0^l EI\left(\frac{d^2f}{dx^2}\right)^2 dx}{\int_0^l m(x) \cdot f^2 dx} = p^2_{изг}$$

gives the natural frequency of the flexural vibrations of the beam at any cross section.

In the case of resonance, we shall have

$$y_{max} = f(x) \frac{A \frac{\partial C_y}{\partial \alpha} \rho V^2 \int_0^l t(x) f(x)\, dx}{\int_0^l m(x) f^2(x) dx \frac{\frac{\partial C_y}{\partial \alpha}\rho V \int_0^l t(x) f^2\, dx}{\int_0^l m(x) f^2(x) dx}\omega} = f(x) \frac{AV \int_0^l t(x) f(x)\, dx}{\omega \int_0^l t(x) f^2\, dx}. \tag{24}$$

But

$$\omega = \sqrt{\frac{\int_0^l EI\left(\frac{d^2f}{dx^2}\right)^2 dx}{\int_0^l m f^2\, dx}}. \tag{25}$$

hence equation (24) can be written in the form

$$y_{max} = f(x) \frac{A \cdot V \int_0^l t(x) f(x)\, dx}{\int_0^l t(x) \cdot f^2\, dx \sqrt{\frac{\int_0^l EI\left(\frac{d^2f}{dx^2}\right)^2 dx}{\int_0^l m(x) f^2(x)\, dx}}}. \tag{26}$$

For $EI = \text{const}_1$; $m(x) = \text{const}_2$; $t(x) = \text{const}_3$; we obtain

$$y_{max} = \frac{f(x)A\ Vt \int_0^l f(x)dx}{t \int_0^l f^2(x)dx \sqrt{\frac{\int_0^l \left(\frac{d^2f}{dx^2}\right)^2 dx}{\int_0^l f^2 dx} \sqrt{\frac{EI}{m}}}} = \frac{\text{const } fV}{\sqrt{\frac{EI}{m}}}$$

that is, the same result is obtained as by the usual classical solution by the method of Poisson. The simplicity of the obtained formula is such that no explanations with regard to the value of the individual parameters are required. It is important to note only one point; namely, that in the case of resonance the values of the deflections do not depend on the aerodynamic properties of the tail itself. This result follows from the assumption of the stationary theory.

Case of Purely Torsional Vibrations

In the case of purely torsional vibrations, the above line of reasoning remains exactly the same as for the purely flexural vibrations. We shall present only the final result.

The equation of motion for torsional vibration is of the form

$$-\frac{\partial}{\partial x}\left(GI_p\frac{\partial\theta}{\partial x}\right) + I_m\frac{\partial^2\theta}{\partial\tau^2} - \frac{\partial C_{mE}}{\partial\alpha}\rho V^2t^2\left[\theta + \frac{t}{V}\left(\frac{3}{4} - \frac{x_o}{t} + \frac{\pi}{16\frac{\partial C_{mE}}{\partial\alpha}}\right)\frac{\partial\theta}{\partial\tau}\right] = M(x)\sin\omega\tau \qquad (27)$$

Setting

$$\theta = \varphi(x)\ \zeta(\tau) \qquad (28)$$

and applying the method of Galerkin, we obtain

$$\theta = \varphi(x)\frac{\int_0^l M(x)\varphi(x)dx \sin(\omega\tau + \epsilon)}{\sqrt{\left[\int_0^l GI_p\left(\frac{d\varphi}{dx}\right)^2 dx - \int_0^l \frac{\partial C_{mE}}{\partial\alpha}\rho V^2t^2\varphi^2\,dx - \omega^2\int_0^l I_m\varphi^2\,dx\right]^2 + \psi^2}} \qquad (29)$$

where

$$\psi = \omega\left[\int_0^l \frac{\partial C_{mE}}{\partial \alpha}\rho\, Vt^3\left(\frac{3}{4} - \frac{x_o}{t} - \frac{\pi}{16\frac{\partial C_m}{\partial \alpha}}\right)\varphi^2\, dx\right]$$

As is seen from formula (29), the aerodynamic characteristics of the tail surface itself affect the character of the vibrations. In the first place, there is a decrease in the natural frequency of the vibrations by the amount

$$\frac{\rho\, V^2\int_0^l \frac{\partial C_{mE}}{\partial \alpha}\, t^2\, \varphi^2\, dx}{\int_0^l I_m \varphi^2\, dx}$$

that is, there is a drop also in the velocity at which resonance appears. In the second place, in the case of resonance itself the deflections, in contrast to those of the flexural vibrations, will depend on the aerodynamic characteristics of the tail section, as is shown by equation (29).

III. THE CASE OF TWO DEGREES OF FREEDOM

As is known from the theory of wing vibration, vibrations of a wing with one degree of freedom are impossible, the flexural vibrations necessarily giving rise to torsional vibrations and vice versa, that is, the tail surface vibrations will always be torsional-flexural. This is due to the noncoincidence of the points of application of the elasticity and inertia forces. It is a question only of the relative importance of each of these types of vibrations in the general system of vibration. We shall therefore consider the motion for the case of two degrees of freedom, that is, simultaneous vibration in torsion and bending.

The system of equations is of the form

$$\frac{\partial^2}{\partial x^2}\left(EI(x)\frac{\partial^2 y}{\partial x^2}\right) + m(x)\frac{\partial^2 y}{\partial \tau^2} - m\sigma\frac{\partial^2 \theta}{\partial \tau^2}$$

$$- \frac{\partial C_y}{\partial \alpha}\rho\, V^2 t\left[\theta + \frac{t}{V}\left(\frac{3}{4} - \frac{x_o}{t}\right)\frac{\partial \theta}{\partial \tau} - \frac{1}{V}\frac{\partial y}{\partial \tau}\right] = p(x)\sin \omega\tau; \qquad (30)$$

$$- \frac{\partial}{\partial x}\left(GI_p \frac{\partial \theta}{\partial x}\right) - m\sigma \frac{\partial^2 y}{\partial \tau^2} + I_m \frac{\partial^2 \theta}{\partial \tau^2}$$

$$- \frac{\partial C_{m\epsilon}}{\partial \alpha} \rho V^2 t^2 \left[\theta + \frac{t}{V}\left(\frac{3}{4} - \frac{x_o}{t} - \frac{\pi}{16 \frac{\partial C_{m\epsilon}}{\partial \alpha}}\right)\frac{\partial \theta}{\partial \tau} - \frac{1}{V}\frac{\partial y}{\partial \tau}\right] = \gamma(x) \sin \omega\tau \qquad (31)$$

where

$$p(x) = A\frac{\partial C_y}{\partial \alpha} \rho V^2 t(x); \qquad \gamma(x) = A\frac{\partial C_{m\epsilon}}{\partial \alpha} \rho V^2 t^2(x)$$

This system of two linear partial differential equations may be integrated only approximately. As has already been pointed out, the difficulty of integrating nonhomogeneous equations is the same as that for homogeneous, since the problem in both cases reduces to finding the functions $y(x)$, $\varphi(x)$ and expanding them in absolutely and uniformly converging series in each case. The solution of this system, we shall seek, in the form

$$y = f(x)\,\xi(\tau); \qquad \theta = \varphi(x)\,\psi(\tau) \qquad (32)$$

Substituting these functions in the equations and multiplying the first by $f(x)dx$, the second by $\varphi(x)dx$ and integrating from 0 to l, we obtain

$$\left.\begin{aligned} a_{11}\xi + a_{12}\ddot{\xi} + a_{13}\ddot{\psi} + a_{14}\psi + a_{15}\dot{\psi} + a_{16}\dot{\xi} &= a \sin \omega\tau \\ b_{11}\psi + b_{12}\ddot{\xi} + b_{13}\ddot{\psi} + b_{14}\psi + b_{15}\dot{\psi} + b_{16}\dot{\xi} &= b \sin \omega\tau \end{aligned}\right\} \qquad (33)$$

where

$$a_{11}=\int_0^l EI\left(\frac{d^2f}{dx^2}\right)^2 dx; \qquad a_{12}=\int_0^l m(x)f^2\,dx; \qquad a_{13}=-\int_0^l m\sigma f(x)\,dx;$$

$$a_{14}=-\frac{\partial C_y}{\partial\alpha}\rho V^2\int_0^l t\varphi(x)f(x)\,dx; \qquad a_{15}=-\frac{\partial C_y}{\partial\alpha}\rho V\int_0^l t^2\left(\frac{3}{4}-\frac{x_0}{t}\right)\varphi(x)\cdot f(x)\,dx;$$

$$a_{16}=\frac{\partial C_y}{\partial\alpha}\rho V\int_0^l tf^2\,dx; \qquad a=\int_0^l p(x)f(x)\,dx; \qquad b_{11}=\int_0^l GI_p\left(\frac{d\varphi}{dx}\right)^2 dx;$$

$$b_{12}=\int_0^l m\sigma f(x)\,dx; \qquad b_{13}=\int_0^l I_m\varphi^2\,dx; \qquad b_{14}=-\rho V^2\int_0^l\frac{\partial C_{m_\varepsilon}}{\partial\alpha}t^2\varphi^2\,dx;$$

$$b_{15}=-\rho V\int_0^l\frac{\partial C_{m_\varepsilon}}{\partial\alpha}t^3\left(\frac{3}{4}-\frac{x_0}{t}-\frac{\pi}{16\dfrac{\partial C_{m_\varepsilon}}{\partial\alpha}}\right)\varphi^2\,dx;$$

$$b_{16}=\rho V\int_0^l\frac{\partial C_{m_\varepsilon}}{\partial\alpha}t^2f(x)\varphi(x)\,dx; \qquad b=\int_0^l\gamma(x)\varphi(x)\,dx.$$

We assume

$$\xi=\overline{A}\cos\omega\tau+\overline{B}\sin\omega\tau; \quad \psi=\overline{C}\cos\omega\tau+\overline{D}\sin\omega\tau,$$

since there is always a phase difference between the forces acting on the tail and its displacements. Substituting these expressions in the obtained equations, we shall have

$$a_{11}(\overline{A}\cos\omega\tau+\overline{B}\sin\omega\tau)+a_{12}(-\omega^2\overline{A}\cos\omega\tau-\omega^2\overline{B}\sin\omega\tau)+$$
$$+a_{13}(-\omega^2\overline{C}\cos\omega\tau-\omega^2B\sin\omega\tau)+a_{14}(\overline{C}\cos\omega\tau+\overline{D}\sin\omega\tau)+$$
$$+a_{15}(-\omega\overline{C}\sin\omega\tau+\omega\overline{D}\cos\omega\tau)+a_{16}(-\omega\overline{A}\sin\omega\tau+\omega\overline{B}\cos\omega\tau)=a\sin\omega\tau;$$
$$b_{11}(\overline{C}\cos\omega\tau+\overline{D}\sin\omega\tau)+b_{12}(-\omega^2\overline{A}\cos\omega\tau-\omega^2\overline{B}\sin\omega\tau)+$$
$$+b_{13}(-\omega^2\overline{C}\cos\omega\tau-\omega^2\overline{D}\sin\omega\tau)+b_{14}(\overline{C}\cos\omega\tau+\overline{D}\sin\omega\tau)+$$
$$+b_{15}(-\omega\overline{C}\sin\omega\tau+\omega\overline{D}\cos\omega\tau)+b_{16}(-A\omega\sin\omega\tau+\omega B\cos\omega\tau)=b\sin\omega\tau.$$

Equating the coefficients before the same functions, we obtain

$$\overline{A}(a_{11}-a_{12}\omega^2)+\overline{B}a_{16}\omega+\overline{C}(a_{14}-a_{13}\omega^2)+\overline{D}a_{15}=0;$$
$$-\overline{A}a_{16}\omega+\overline{B}(a_{11}-a_{12}\omega^2)-\overline{C}a_{15}\omega+\overline{D}(a_{14}-a_{13}\omega^2)=a;$$
$$-\overline{A}b_{12}\omega^2+\overline{B}b_{16}\omega+\overline{C}(b_{11}-b_{13}\omega^2+b_{14})+\overline{D}b_{15}\omega=0;$$
$$-\overline{A}b_{16}\omega-\overline{B}b_{12}\omega^2-\overline{C}b_{15}\omega+\overline{D}(b_{11}-b_{13}\omega^2+b_{14})=b.$$

whence

$$\overline{A} = \frac{\Delta_1}{\Delta}; \qquad \overline{B} = \frac{\Delta_2}{\Delta};$$

$$\overline{C} = \frac{\Delta_3}{\Delta}; \qquad \overline{D} = \frac{\Delta_4}{\Delta}.$$

where

$$\Delta = \begin{vmatrix} a_{11} - a_{12}\omega^2 & a_{16}\omega & a_{14} - a_{13}\omega^2 & a_{15}\omega \\ -a_{16}\omega & a_{11} - a_{12}\omega^2 & -a_{15}\omega & a_{14} - a_{13}\omega^2 \\ -b_{12}\omega & b_{16}\omega & b_{11} - b_{13}\omega^2 + b_{14} & b_{15}\omega \\ -b_{16}\omega & -b_{12}\omega^2 & -b_{15}\omega & b_{11} - b_{13}\omega^2 + b_{14} \end{vmatrix}$$

$$\Delta_1 = \begin{vmatrix} 0 & a_{16}\omega & a_{14} - a_{13}\omega^2 & a_{15}\omega \\ a & a_{11} - a_{12}\omega^2 & -a_{15}\omega & a_{14} - a_{13}\omega^2 \\ 0 & b_{16}\omega & b_{11} - b_{13}\omega^2 + b_{14}\omega & b_{15}\omega \\ b & -b_{12}\omega^2 & -b_{15}\omega & b_{11} - b_{13}\omega^2 + b_{14} \end{vmatrix}$$

$$\Delta_2 = \begin{vmatrix} a_{11} - a_{12}\omega^2 & 0 & a_{14} - a_{13}\omega^2 & a_{15}\omega \\ -a_{16}\omega & a & -a_{15}\omega & a_{14} - a_{13}\omega^2 \\ -b_{12}\omega^2 & 0 & b_{11} - b_{13}\omega^2 + b_{14} & b_{15}\omega \\ -b_{16}\omega & b & -b_{15}\omega & b_{11} - b_{13}\omega^2 + b_{14} \end{vmatrix}$$

$$\Delta_3 = \begin{vmatrix} a_{11} - a_{12}\omega^2 & a_{16}\omega & 0 & a_{15}\omega \\ -a_{16}\omega & a_{11} - a_{12}\omega^2 & a & a_{14} - a_{13}\omega^2 \\ -b_{12}\omega^2 & b_{16}\omega & 0 & b_{15}\omega \\ b_{16}\omega & -b_{12}\omega^2 & b & b_{11} - b_{13}\omega^2 + b_{14} \end{vmatrix}$$

$$\Delta_4 = \begin{vmatrix} a_{11} - a_{12}\omega^2 & a_{16}\omega & a_{14} - a_{13}\omega^2 & 0 \\ -a_{16}\omega & a_{11} - a_{12}\omega^2 & -a_{15}\omega & a \\ -b_{12}\omega^2 & b_{16}\omega & b_{11} - b_{13}\omega^2 + b_{14} & 0 \\ -b_{16}\omega & -b_{12}\omega^2 & -b_{15}\omega & b \end{vmatrix}$$

In the entire discussion above, it was assumed that the functions f(x) and $\varphi(x)$ are known. Actually, their determination presents one of the most difficult problems of present day mathematics. There is a small number of particular cases for which these functions can be given in strict form. In all practical cases, they are generally found by approximate methods and the results later checked by experiment. In the case of forced vibrations there is one advantage; namely, that for the determination of the amplitude it is not required to use the initial conditions without which in the homogeneous problem the amplitude cannot be determined.

As is known, we seek the solution of both the homogeneous and nonhomogeneous equations in the form of the product

$$y = f(x)\zeta(\tau).$$

For $f(x)$, in both of the above cases, there are a sufficient number of boundary conditions, but for ζ in the case of the homogeneous problem it is necessary to specify initial conditions and in the case of the nonhomogeneous problem ζ is entirely determined by the disturbance forces. Thus, multiplication of the right-hand side by any constant factor does not introduce any complications in the determination of the amplitude, and the computation can always be carried through to the end. Thus, it is possible to take $Af(x)$ for $f(x)$, since A can enter in the coefficient ζ.

As a first approximation, we assumed that the form of vibration of the tail in the flow is the same as in the case of vibrations of the same surface in a vacuum. On the basis of these assumptions, the buffeting computation of the tail was made with the data presented in the book of E. P. Grossman (reference 10) on the assumption that the wing chord was equal to 3 meters and the maximum angle of attack that could arise from the effect of the wake was equal to 5° for vibration with two degrees of freedom.

The curves (figs. 6 and 7) of the change of maximum deflections and torsional angles theoretically obtained, show the interesting characteristic which is observed also in practice; namely, that the forced torsional vibrations start only when the frequencies of the disturbing forces approach the frequencies of the natural flexural vibrations of the tail, while the flexural vibrations strongly increase with increase in the flow velocity.

In the light of the theoretical results obtained, it is useful to recall the following fact. In considering the failure of the tail of the JU 13, the English investigators arrived at the conclusion that the failure arose from the flexural stresses. This is indirectly confirmed by the fact that the accident was caused by buffeting since, as shown by the computations, in buffeting the flexural vibrations predominate.

IV. EXPERIMENTAL INVESTIGATIONS OF BUFFETING IN THE LABORATORY AT HIGH REYNOLDS NUMBER

Buffeting investigations were carried out in the wind tunnel on a model of an elastic tail placed in a disturbed

flow behind the wing. The tests were conducted both on an isolated wing and on a combination of wing and fuselage. The model tail surface was a single spar airfoil of symmetric section. As may be seen from the sketch (fig. 8), it is assembled in several sections in such a manner that the entire load is taken only by the spar with the skin taking no load. The model was, moreover, designed in two variants which differed only in the material of the spar, one being of steel and the other of duralumin. This model design was chosen with a view to the requirement, not only of fixing the frequency of vibration but also of determining the order of aerodynamic loads acting on the tail surface. As has already been pointed out, the investigations of foreign laboratories suffered from the fundamental defect that they made use of a detector which having elastic properties very dissimilar to those of the wing could not yield any information with regard to the load. In our case this problem was solved, though very approximately, without disturbing the accuracy with respect to the frequencies. This is entirely understandable since tails working in the region below the stalling velocities will have no free vibrations, but will accurately follow the forced frequencies.

The dimensions of the tail surface are indicated on figure 8. The fuselage was schematically represented by a flat board 30 millimeters thick which was attached directly to the wing forming a right-angle joint.

In order to include the basic practical operating conditions, five such board fuselages were constructed by which settings were obtained to correspond to the angles of attack of the wing of 0.5°, 10°, 15°, and 20°. Moreover, such fuselages, not having any elastic connection with the tail, made possible the determination of only the purely aerodynamic effect of the fuselage on the tail.

A sketch of the setup is shown on figure 9. The vertical position of the tail was chosen after a special test in which the amplitudes of vibration of the tip of the tail were observed for various vertical positions of the tail surface. The plane of the upper edge of the wing gave the maximum amplitude. This agrees entirely with the results of Duncan and the tail was therefore set at the level of the upper edge of the wing.

Test Procedure

The object was to determine the frequency and amplitude of the tail vibration. The problem of the choice of any particular method of obtaining the fundamental parameters depended naturally on the character of the vibrations themselves, that is, whether regular or irregular, observable with the naked eye or not, and finally, on the number of degrees of freedom possessed by the tail. For this purpose, the vibrating tail was observed by stroboscopic illumination. It was found that by a corresponding choice of the stroboscope frequency the vibrations could be completely determined. Moreover, it was found that the tail in the disturbed flow vibrated with considerable amplitude, the vibrations being purely flexural up to a certain definite velocity and after this velocity had been reached, being accompanied by torsional vibrations. This made it possible to photograph the tail surface and to determine the maximum amplitudes from the film. In this way, rather simple and at the same time, sufficiently accurate apparatus was chosen for measuring the fundamental parameters; namely, the rotoscope for measuring the frequencies and the usual photographic apparatus for the amplitudes.

Results of Observations

The observations showed that at all angles of attack of the wing when there was no separation of flow the tail did not vibrate. For the case of an isolated wing, for example, the tail vibrations started at $\alpha_w > \alpha_{w\,cr}$. In this case the tail vibrated at all flow velocities, increasing with increase in the latter, the vibrations being predominantly flexural. Torsional vibrations arise only when the frequencies of the flow approach the flexural frequencies of the tail, there being practically no torsional vibrations up to this moment, as was shown theoretically.

Figure 10 shows the curves of frequency against velocity. As may be seen, the points with sufficient accuracy lie on a straight line. It should be noted that the straight line of ν against V does not pass through the origin of coordinates. This shows that at small velocities the law of variation of ν with V will be different than in the given case. We shall write the equation of this straight line

$$\nu = \nu_0 + k(V - V_0)$$

where ν_o, V_o are the initial frequency and velocity of the flow.

Dividing both sides of the equation by V we obtain

$$\frac{\nu}{V} = \frac{\nu_o}{V} + k - \frac{V_o}{V}$$

from which it is seen that for large values of the velocity the ratio ν/V is simply equal to k, the slope of the line. From the value of k taken from the curve of figure 10 we compute $S_t = 0.1$. For actual landing velocities the value of S_t may be taken approximately equal to $0.115 \div 0.12$. It is evident that these results may be made more accurate when tests for the determination of S_t are conducted for a large number of full-scale wings.

On figure 11 is plotted ν/V against V. The fact that the measurements obtained by the stroboscopic method qualitatively agree with the results of other authors lends support to the assumption of full periodicity of the disturbance forces behind the isolated wing. This is a very important fact for the problem of buffeting. If the forces were not periodic it would not have been possible to apply the stroboscope which operates according to the harmonic law. Logically, it could not be expected otherwise, for with a given wing and at a given velocity, that is, for constant conditions of stall, the time required for the full stalling process should not change.

The curves of change of amplitude with velocity confirm the conclusions previously drawn since all the curves show definite resonance states as would be impossible in the case of irregularity of the disturbance forces since the natural tail vibrations are harmonic.

Figure 12 shows the curve of amplitude against velocity for $\alpha_w = 26^\circ$ and $\alpha_t = 0$, 5°, and 10°. The curves for $\alpha_t = 0$ and 5° are of a character corresponding to the general theory of forced vibrations. For $\alpha_t = 10^\circ$ the curve differs sharply from the preceding since the stalling point is at $\alpha_t \cong 11^\circ$. It appears that a change in angle of attack in the wake behind the wing alternately brings the wing from the condition above to the condition below the stall, and this explains the arbitrary character of the curve.

Figure 13 likewise shows a sharp difference in the behavior of the curves for $\alpha_t = 0^\circ$ and $\alpha_t = 10^\circ$. Whereas for $\alpha_t = 0^\circ$ the amplitude curve has its maximum value; its minimum value is $\alpha_t = 10^\circ$. This is apparently due to the decrease in the amplitude of the forces acting on the tail as a result of the transition of the tail surface to the conditions beyond the stall. Figure 13 shows the results characterizing the behavior of the tail behind a wing with larger chord than for the first case, that is, figure 14. For this reason, resonance is reached at larger values of the velocity. Figure 14 shows comparison curves for two tail surfaces with different stiffness. These curves show that a simple change in the stiffness not only changes the numerical value of the amplitudes but also sharply modifies the character of the vibration. For this reason, the question of stiffness is of fundamental importance in the buffeting theory.

An increase in the wing dimensions and in its angle of attack has a great effect on the amplitude of the vibrations. Figure 15 gives the results of tests on a wing of chord 0.63 meter at $\alpha_w = 30^\circ$ (tail with steel spar) which show that the increase in the amplitude with the velocity follows, approximately, the cubic law.

Combination of Wing and Fuselage

As has already been stated, boards attached to the wing forming a right-angle intersection were used as fuselages, five fuselages being used to form models with wing angle of attack of 0°, 5°, 10°, 15°, and 20°. This made it possible to include the entire range of practical angles of attack.

From the work of a number of authors it has been established that the initial separation of the flow due to the interference between the wing and fuselage often starts at a wing angle of attack of 2° to 3° in the case of intersections without fairings. We were guided by these facts in choosing such a number of angles of attack for investigation.

When the tests were begun it was found that up to $\alpha_w = 15^\circ$ inclusive, the tail surface does not vibrate and the silk string shows the absence of separation at the intersection. Only at $\alpha_w = 15^\circ$ and at large velocities is there formed at the wing and fuselage intersection a

small breakdown region and slight vibration of the tail. This is explained, evidently, by the straight line character of the contour of our fuselage, that is, by the absence of a pressure drop in the flow along the fuselage. The fuselage and wing having different profiles form different velocity vectors at the same points of space in the region of the intersection. This leads to a disturbance of the smoothness of the flow about the wing and fuselage. In our case, the fuselage, not having any pressure gradient and hence variable velocities along the contour, does not disrupt the flow at the wing. We speak here of the outer flow, of course, as the boundary layer in the region of the juncture undoubtedly increases in thickness in the flow direction, but this, evidently, for such type of intersections, plays no important part up to stalling angles of attack. For $\alpha_w = 20^\circ$ the tail vibrates, as in the case of the isolated wing, in the range beyond the stall.

Figures 10 to 16 show the frequencies and amplitudes plotted against the velocity in comparison with the same curves for the isolated wing. As may be seen, the very interesting result is obtained that while the frequencies are not affected by the presence of the fuselage the amplitudes are strongly decreased. This means that the fuselage acts as a damping device for the tail. Thus the presence of the fuselage itself, from the point of view of buffeting, not only plays a negative part, creating vortices at the intersection but also a positive part in damping the vibrations.

V. FORCES ACTING ON THE TAIL IN BUFFETING

We shall try to answer the question with regard to the loads to which the horizontal tail surface is subjected in buffeting. We shall first consider the following simple problem. Let a single vortex with circulation Γ and with a forward velocity equal to the flow velocity move in an infinite ideal flow about a horizontal tail of constant chord. Assuming the path of the vortex as a straight line, the scheme will be that shown in figure 17

where

0 is the initial position of the vortex

S_0 the distance of the tail from the point 0 in the flow direction

h_0 is the distance of the tail from O along the vertical

S the running coordinate of the vortex

The vortex will, of course, induce at the tail the velocity vector ΔV which will vary both in magnitude and direction in the course of motion of the vortex. It is required to find the lift force on the tail in this case.

We consider the expression for the lift in the general case of forward motion. The lift, as is known, is given by

$$P = \frac{\rho\pi t}{4}\left[t\frac{d(V\alpha)}{d\tau} + 4V^2\alpha - \frac{2V}{\pi}\int_{\overline{x_0}}^{x}\frac{u(\beta)d\beta}{\sqrt{(x-\beta_0)^2 + t(x-\beta_0)}}\right] \quad (34)$$

where $u(\beta)$ is the intensity of the vortex sheet springing from the trailing edge and generated by lines of velocity discontinuity. In the case of nonstationary motion the circulation at the tail varies and therefore, in order to satisfy Kelvin's theorem of the constancy of the circulation in time, it is necessary that a vortex be shed with circulation equal to the increment in circulation about the tail but of opposite sign. Schematically this may be represented as shown in figure 18, where

$\overline{x_0}$ is the starting point of the nonsteady motion

$\overline{x}$ the distance traversed after the start of the motion

β the running coordinate

Formula (34) thus consists of two parts: namely, the Joukowsky terms and the terms due to the nonstationary character of the motion. As shown by Wagner (reference 11), the value of the latter integral is small by comparison with the remaining terms and may be neglected without too great an error. Moreover, it always acts to reduce the total lift force so that neglecting it will be on the favorable side as regards the wing strength.

In general, $u(\beta)$ is found from the solution of an integral equation of the form

$$V \sin \alpha = \frac{1}{\pi} \int_{\overline{x_0}}^{\overline{x}} \frac{\sqrt{1 + x - \beta}}{\sqrt{x - \beta}} u(\beta) \, d\beta$$

It remains to consider the term $\frac{d(V\alpha)}{d\tau}$. We write it in the form

$$\frac{d(V\alpha)}{d\tau} = V \frac{d\alpha}{d\tau} + \alpha \frac{dV}{d\tau} \tag{35}$$

Assuming the velocity of the flow constant we obtain

$$\frac{d(V\alpha)}{d\tau} = V \frac{d\alpha}{d\tau}$$

The lift force will then be

$$P = \frac{\rho \pi t}{4} \left(t \frac{d\alpha}{d\tau} V + 4 V^2 \alpha \right)$$

It is necessary to determine $\frac{d\alpha}{d\tau}$. From a consideration of figure 17 we may write

$$\alpha = \frac{\Delta V \cos \gamma}{V} = \frac{\Delta V (S_0 - S)}{V \sqrt{(S_0 - S)^2 + h_0^2}} \tag{36}$$

but

$$\Delta V = \frac{\Gamma}{2\pi r} = \frac{\Gamma}{2\pi \sqrt{(S_0 - S)^2 + h_0^2}} \tag{37}$$

Substituting the above in (36) we obtain

$$\alpha = \frac{\Gamma}{2\pi V} \frac{S_0 - S}{(S_0 - S)^2 + h_0^2} \tag{38}$$

whence

$$\frac{d\alpha}{d\tau} = \frac{\Gamma}{2\pi V} \frac{\left[+2(S_0 - S)^2 - (S_0 - S)^2 - h_0^2 \right] \frac{dS}{d\tau}}{\left[(S_0 - S)^2 + h_0^2 \right]^2}$$

but $\frac{dS}{d\tau} = V$.

$$\frac{d\alpha}{d\tau} = \frac{\Gamma}{2\pi} \frac{(S_o - S)^2 - h_o^2}{[(S_o - S)^2 + h_o^2]^2} \tag{39}$$

Since we are interested only in the maximum value of the lift force we shall find the value of S for which $\frac{d\alpha}{d\tau}$ will be a maximum for which purpose we differentiate (39) with respect to S denoting $\frac{d\alpha}{d\tau}$ by $\dot{\alpha}$:

$$\frac{d\dot{\alpha}}{dS} =$$

$$\frac{\Gamma}{2\pi} \frac{-[(S_o-S)^2+h_o]^2\,2(S_o-S)+2\,[(S_o-S)^2+h_o^2]2(S_o-S)\,[(S_o-S)^2-h_o^2]}{[(S_o-S)^2+h_o^2]^4}$$

Equating the numerator to zero we obtain

$$[(S_o-S)^2+h_o^2]2(S_o-S)=[(S_o-S)^2-h_o^2]4[(S_o-S)^2+h_o^2](S_o-S)$$

$$(S_o-S)^2+h_o^2 = 2(S_o-S)^2-2h_o^2$$

$$S_o-S= \pm \sqrt{3}\, h_o \tag{40}$$

Substituting (40) in (39)

$$\left(\frac{d\alpha}{d\tau}\right)_{max} = \frac{\Gamma}{16\pi h_o^2} \tag{41}$$

But Γ is connected with the angle of attack by the following expression

$$\Gamma = 2\pi V\alpha \frac{(S_o-S)^2+h_o^2}{S_o-S} \tag{42}$$

whence

$$\Gamma = \frac{8\pi}{\sqrt{3}} V h_o\, \alpha \tag{43}$$

Substituting the above in (41)

$$\left(\frac{d\alpha}{d\tau}\right)_{max} = \frac{1}{2\sqrt{3}h_o} V\alpha \tag{44}$$

The expression for the maximum lift force is written as

$$P_{max} = \frac{\rho\pi t}{4}\left(4V^2\alpha + tV\frac{1}{2\sqrt{3}h_o}V\alpha\right) = \rho\pi tV^2\alpha + \frac{1}{8\sqrt{3}}\rho\pi tV^2\alpha\frac{t}{h_o} \quad (45)$$

$$P_{max} = P_{st}\left(1 + \frac{1}{8\sqrt{3}}\frac{t}{h_o}\right) \quad (46)$$

where P_{st} is the lift for steady motion.

The result is thus obtained that the lift of the tail depends on the distance from the vortex lines. The nearer the tail is to the vortex lines the greater the lift force on it for the same angle of attack. It is clear that the case $h_o = 0$ has no immediate physical significance as the tail can never be situated in this position in view of the fact that the tail in turn induces at the vortex a velocity which causes the vortex to deviate, a fact which for simplicity we neglected to take into consideration. Figure 19 shows the curves of vibration amplitude against the vertical position of the tail. It is seen that the maximum deviations lie in the plane of the upper edge of the wing in the flow direction. This may be explained by the fact that the vortices shed from the upper edge of the wing travel approximately in the same plane, a fact which well confirms the assumption made.

On the basis of the obtained formula and the experiments of Duncan it may be stated that the separating vortex travels along a practically straight line. The difficulty may arise that vortices are shed not only from the upper edge of the wing but also from the lower but no such increase in the amplitude of the vibration is obtained in the plane of the lower edge. The reason is that the vortices springing from the upper and lower edges do not produce the same effect on the tail. Having oppositely directed circulations one of the vortices acts to reduce the dynamic load while the other acts to increase it. The theorem is proved in mechanics that for dynamic loading the deformations may attain double the value of those for static load but for dynamic unloading they can never exceed the static load deformations. In general the tail may be loaded not only by the vortices springing from the upper edge but by those from the lower edge depending on the angle of attack of the tail itself. In the given tests due to the downwash of the flow behind the wing the tail was at a negative angle of attack. Hence it would be more correct

to say that the line of dangerous buffeting lies in the plane of the edges of the wing if it is assumed that the vortices travel approximately in these planes in the flow direction.

Figures 20 to 26 give the force curves obtained from the tests. As has already been pointed out the maximum value of the deflections was determined by a photographic camera and from these values the forces were determined by formula (23). Setting $k(x) = A \frac{\partial C_y}{\partial \alpha}$ we obtain

$$k(x) = \frac{y_m \int_0^l m(x) f^2(x)\,dx \sqrt{\left(\frac{\int_0^l EI \left(\frac{d^2 f(x)}{dx^2} \right)^2 dx}{\int m(x) f^2(x)\,dx} - \omega^2 \right)^2 + \left(\frac{\frac{\partial C_y}{\partial \alpha} \rho V \int_0^l t\, f^2(x)\,dx}{\int_0^l m(x) f^2(x)\,dx} \omega \right)^2}}{f(x)\, \rho^2 V \int_0^l t(x) f(x)\,dx}$$

whence

$$\Delta P = k(x)\, \rho V^2 S_t$$

where S_t is the area of the tail surface and y_m the measured amplitude of the tip of the tail. We make use of nondimensional coefficient

$$C = \frac{\Delta P}{C_{y_{max}} \rho V^2 S_t} = \frac{k(x)}{C_{y_{max}}} \text{ 100 percent}$$

The curves show that the variation of the acting forces with the velocity for all cases considered is subject to a definite law. The coefficient C assumes various values not always regular. This is explained partly by the fact that a sinusoid does not accurately represent the actual character of the varying forces which act impulsively and strictly speaking should be represented by a Fourier series. As may be seen the overloads may reach 100 percent and more depending on the characteristics of the wake and the angle of attack of the tail. Theoretically the overloads can be of any order of magnitude from 0 to ∞. The theory is here important on account of the fact that it gives an explanation of the causes giving

rise to these loads since the results of the usual wind tunnel tests and of the Joukowsky theory do not throw any light on the causes giving rise to these overloads. A fundamental factor the effect of which is considered by the theory here presented is the rate of change of the angle of attack of the tail. A vortex traveling toward the tail does not simply vary the angle of attack but does this at a definite rate which is determined by the magnitude of the flight velocity, the circulation of the vortex and the disposition of the tail surface relative to the vortex path. The physical theory concerns itself with the explanation of the effect of these factors. The infinite increase in the force for $h_o = 0$ must be considered as the maximum overload of the tail surface in this position, similar to the infinite velocity at the sharp edges in the case of the wing theory.

CONCLUSION

We have considered a very simplified scheme of a complicated phenomenon which is often a source of worry to designers and which up to the present has received no fundamental solution. In this very simple scheme it was found that the isolated wing gives rise to purely periodic disturbances which can be represented by a simple series of trigonometric functions. It is shown that the tail too vibrates periodically with amplitudes increasing with the velocity corresponding to the laws of the general theory of forced vibrations in a resisting medium.

Consideration was given to the character of the loads to which the tail surface was subjected in the wake of the wing. It was found that they are fundamentally determined by

a) The ratio of the frequency of the flow to the natural frequency of the tail surface;

b) The magnitude of the flow velocity

c) The vertical position of the tail surface relative the wing

d) The amplitude of the disturbance forces

Depending on the character of the combination of all these factors the tail may be brought into a critical buffeting condition and in this connection the conclusion of Blenk with regard to the impossibility of failure of the Junkers Ju 13 due to buffeting does not appear to be an entirely justified assertion. At the value S_t = 0.12 obtained in our tests the Junkers airplane was in a resonance state at large velocities, that is, simultaneous action of the above factors a and b was obtained.

The actual character of the tail vibration on a real airplane is very complicated, a fact which is quite understandable since it is not a question of the tail vibrations alone but of the vibrations of the complete mechanical system including a very large number of the structural details.

The important question is how to eliminate buffeting on the actual airplane. Experiment shows that a very large number of structural details of a size comparable with that of the tail surface may form a disturbing wake acting on the tail surface and giving rise to buffeting at various velocities of the airplane. The factor of comparable size is here emphasized since for some reason it is customary to assume in usual practice that even a small bolt on the upper surface of the wing may give rise to dangerous buffeting. In a wind tunnel at $\alpha_w = 10^\circ$ on a wing of 600-millimeter chord plastic objects of various shapes of dimensions 100 to 150 millimeters were attached and no buffeting was observed. This is explained by the fact that the frequencies of the vortices springing from such small objects many times exceed the natural frequency of the tail and their amplitudes in the first place are small in magnitude and in the second place do not reach the tail, being dissipated completely by diffusion. In order to check this the following test was made. A plate of 125 millimeters width was placed ahead of the tail the latter vibrating with appreciable amplitude. These vibrations decreased with increasing distance from the plate and at a distance of about 1 millimeter from the tail they vanished completely.

Thus in considering the origin of the buffeting it is necessary to pay attention to structural details of a greater order of magnitude than small excrescences. If buffeting occurs in landing the source of the trouble in most cases is to be found in the wing attachment to the

fuselage. The measures to be taken for eliminating buffeting in this case are well known to all designers (the use of various kinds of a fairings, slats, flaps, etc., the action of which leads either to a suppression of the flow breakdown at the intersection or to a reduction of the likelihood of resonance between the vortices and tail. It is here necessary to bear in mind first that fillets often have an unfavorable effect on the speed characteristics of the airplane, and secondly that buffeting arising in the presence of fillets often is more dangerous than without them. This is well illustrated on the curves of Duncan (fig. 27) which give the changes in amplitude for various combinations of fillets with other types of devices.

In general the means taken for eliminating buffeting may be classified into three groups:

1. Removal of the causes producing buffeting, that is, avoidance of the possibility of flow breakdown at the wing.

2. Location of the tail in the least dangerous position.

3. Change in the elastic properties of the tail so that its natural frequencies will not be resonance frequencies.

The first group has already been discussed. The second group requires that the tail surface be located as far as possible from the path of the vortices which lie approximately in the plane of the wing edges. This can always be done by sketching the path of the vortices on the drawing for various angles of attack and taking account of the actual conditions of flow about a given wing system.

The means for eliminating buffeting included in the third group are very often applied in practice in the final design of an airplane. It is necessary in many cases to vary the postion of the tail surface several times or strengthen it by various supports which is often done blindly without any preliminary computations. The values of S_t given in the present paper would seem to offer a certain usefulness to the designer by enabling him to determine in advance the required order of natural

frequencies of the tail surface, that is, its elastic properties.

Translation by S. Reiss,
National Advisory Committee
for Aeronautics.

REFERENCES

1. Blenk, Hermann, Hertel, Heinrich, and Thalau, Karl: The German Investigation of the Accident at Meopham (England). T.M. No. 669, NACA, 1932.

2. Duncan, W. J., Ellis, D. L., and Scruton, C.: First Report on the General Investigation of Tail Buffeting. R. & M. No. 1457, British A.R.C., 1932.
Duncan, W. J., Ellis, D. L., and Smyth, E.: Second Report on the General Investigation of Tail Buffeting. R. & M. No. 1541, British A.R.C., 1933.

3. White, James A., and Hood, Manley J.: Wing—Fuselage Interference, Tail Buffeting, and Air Flow about the Tail of a Low—Wing Monoplane. Rep. No. 482, NACA, 1934.

4. Biechteler: Versuche zur Beseitung von Leitwerksschütteln. Z.F.M., No. 1, 1935.

5. Strouhal: Über eine besondere Art der Tonerregung. Annalen der Physik und Chemie, Neue Folge, Bd. V, 1878, pp. 216—251.

6. Fage, A., and Johansen, F. C.: On the Flow of Air Behind an Inclined Flat Plate of Infinite Span. R. & M. No. 1104, British A.R.C., 1927.

7. Blenk, H., Fuchs, D., and Liebers, F.: Über Messungen von Wirbelfrequenzen. Luftfahrtforschung. Bd. 12, No. 1, March 28, 1935, pp. 38—41.

8. Relf, E. F., and Simmons, L. F. G.: The Frequency of the Eddies Generated by the Motion of Circular Cylinders Through a Fluid. R. & M. No. 917, British A.R.C., 1924.

9. Petersohn, E.: Downwash Measurements Behind Wings With Detached Flow. T.M. No. 632, NACA, 1931.

10. Grossman, E. P.: Flutter. CAHI Rep. 284, 1937.

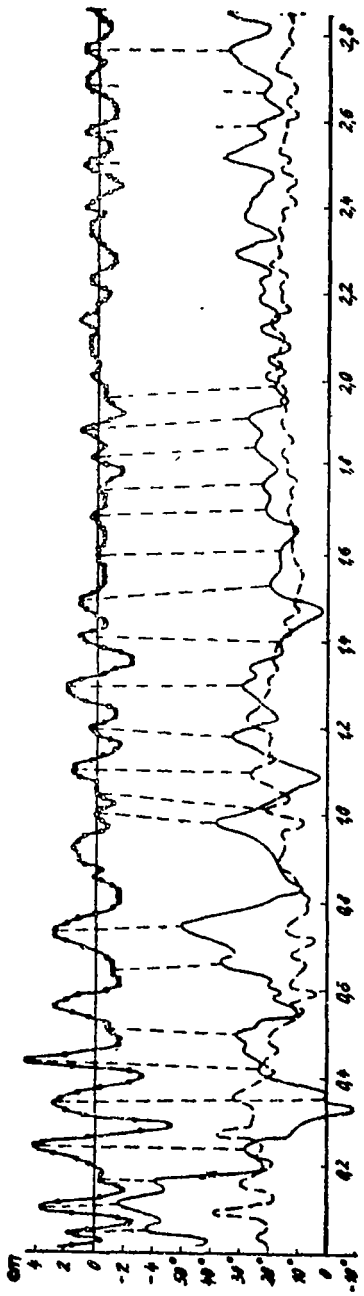

Figure 1.- Vibration of tail and silk thread during gliding of the airplane. Ordinates give deflection of the tip of the stabilizer and angles of inclination of thread. Abscissas give time in seconds. —○—○— horizontal tail surface; ———— outer silk threads; ———— inner silk threads.

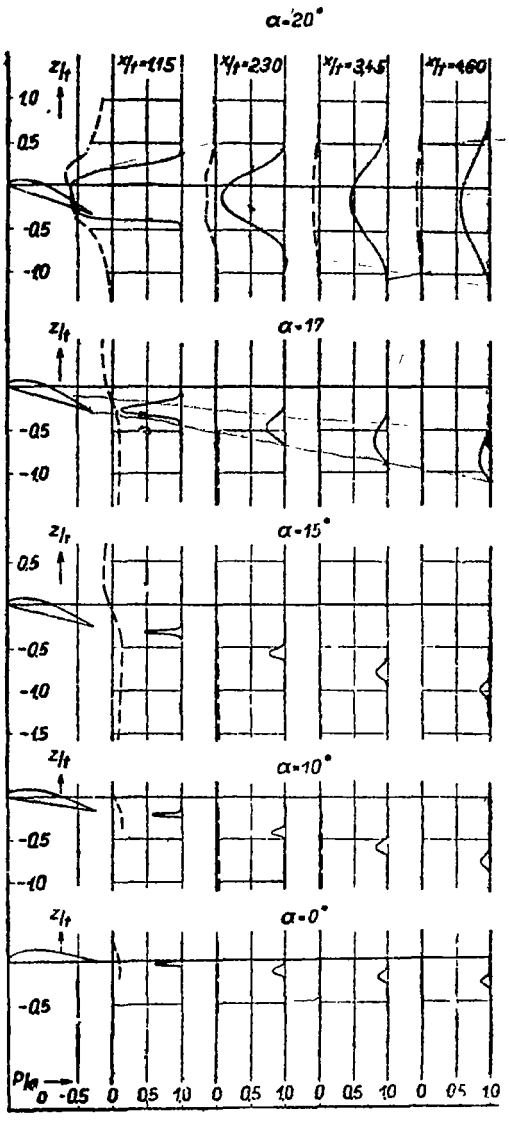

Figure 3.- Graphs of wake behind a wing profile. ———— total pressure; - - - - - - static pressure; t chord; x distance along horizontal; z distance along vertical.

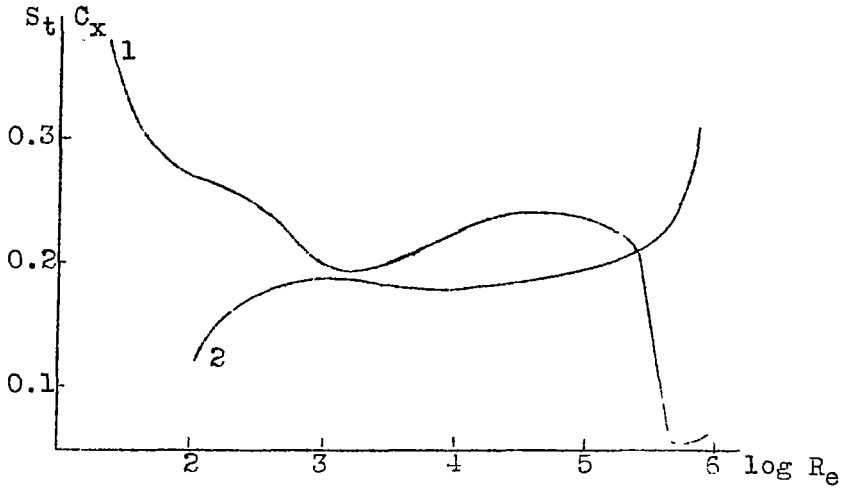

Figure 2.- Curves of S_t and C_x against R_e.

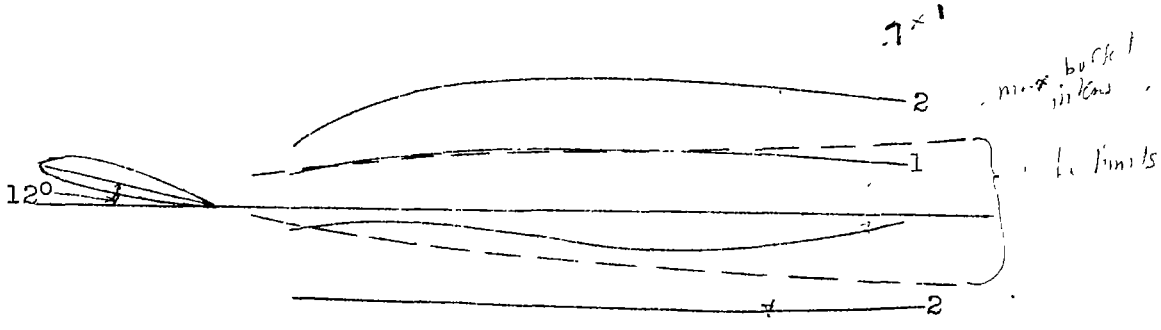

Figure 4.- Comparison of wakes obtained with a pitot tube and a "detector".

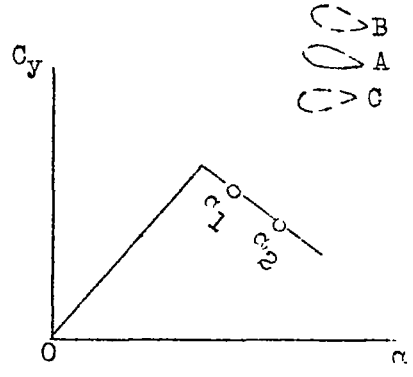

Figure 5.- Curve of C_y against α.

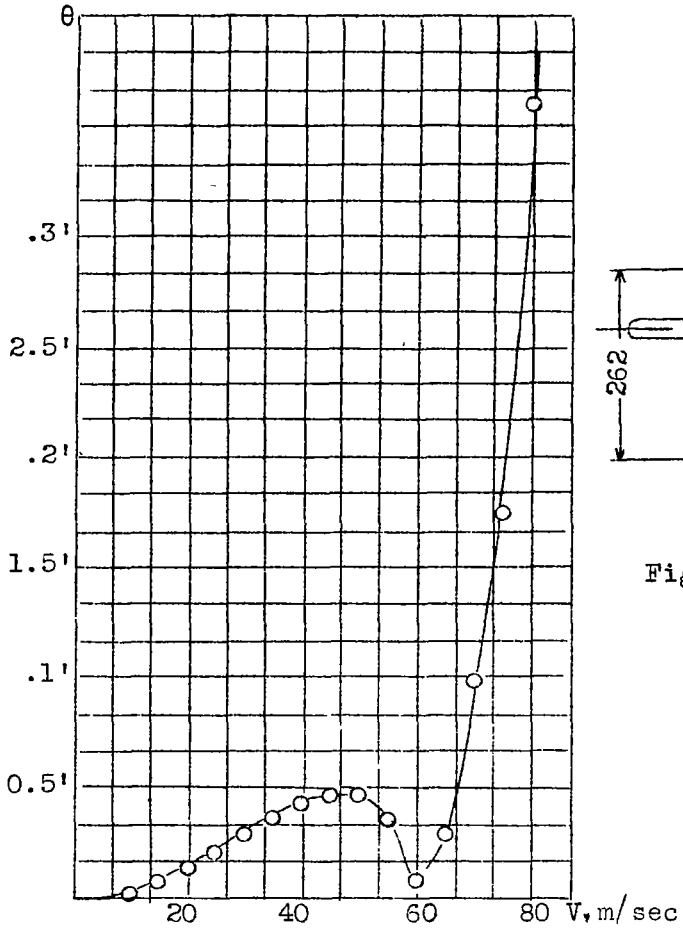

Figure 6.- Maximum angles of twist of tip of tail.

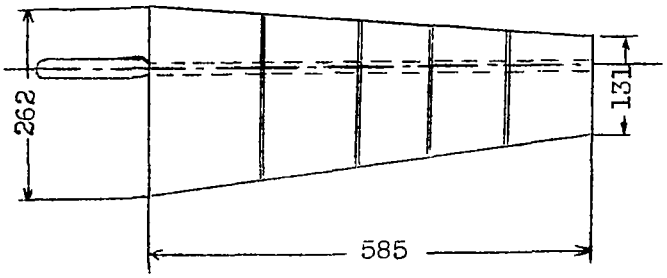

Figure 8.- Sketch of model tail.

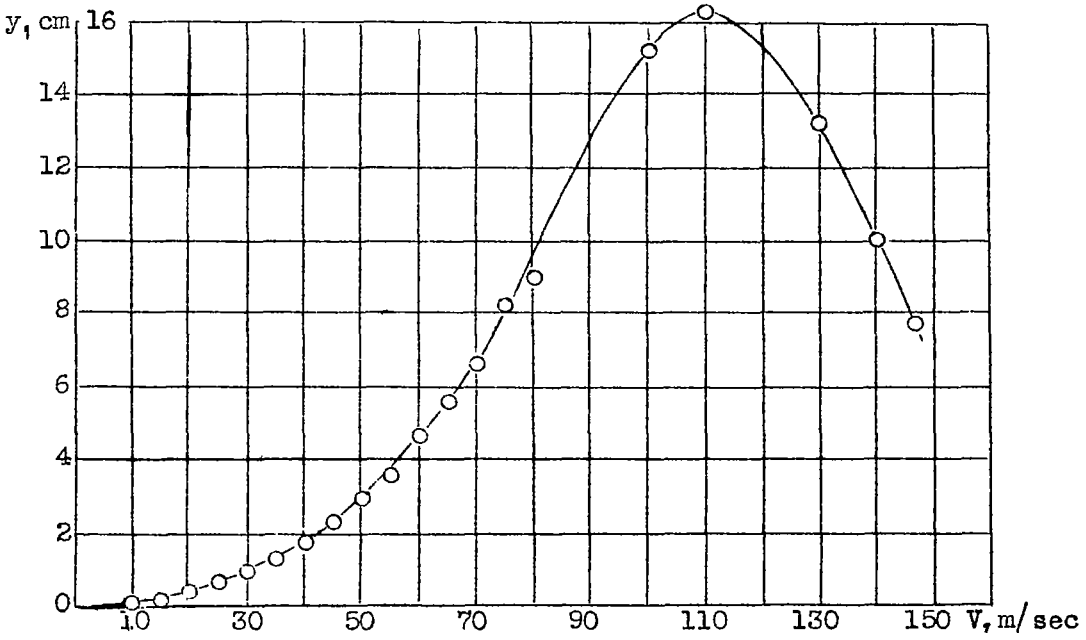

Figure 7.- Maximum deflections of tip of tail.

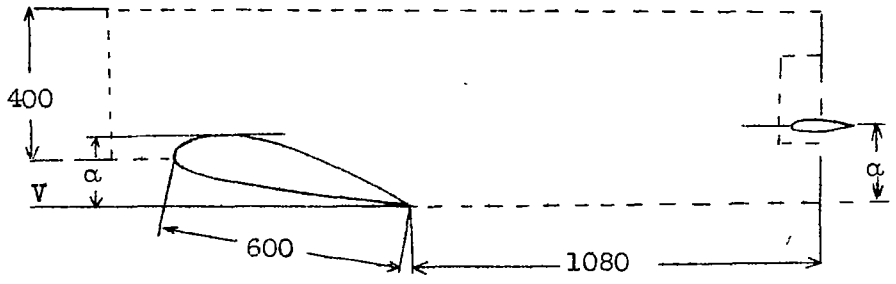

Figure 9.- General set-up. Dotted line indicates the board fuselage.

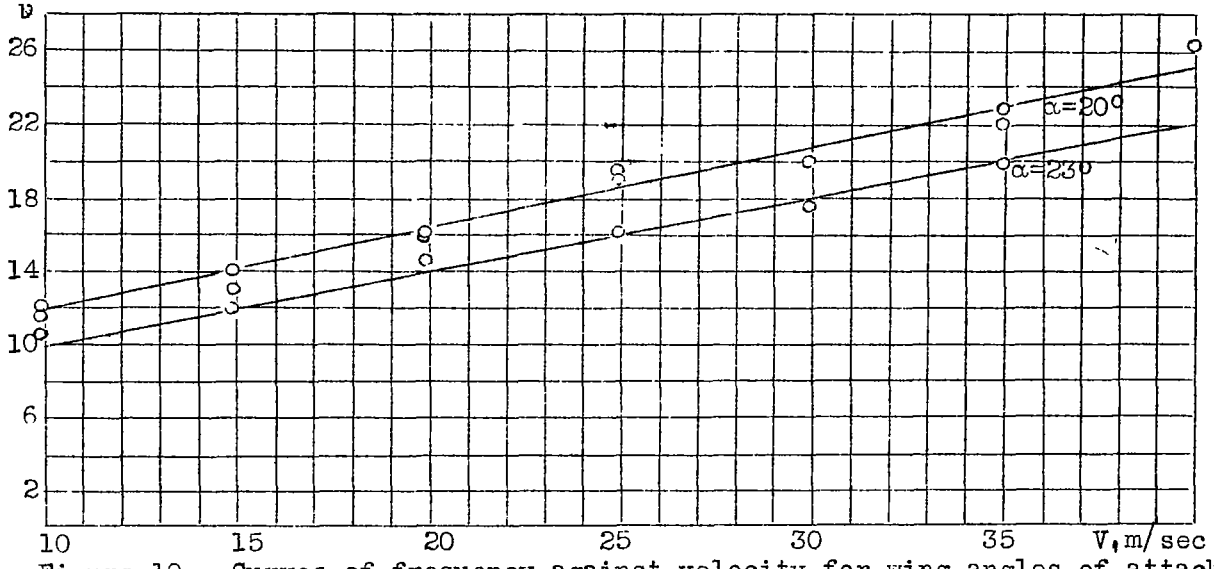

Figure 10.- Curves of frequency against velocity for wing angles of attack of 20° and 23°.

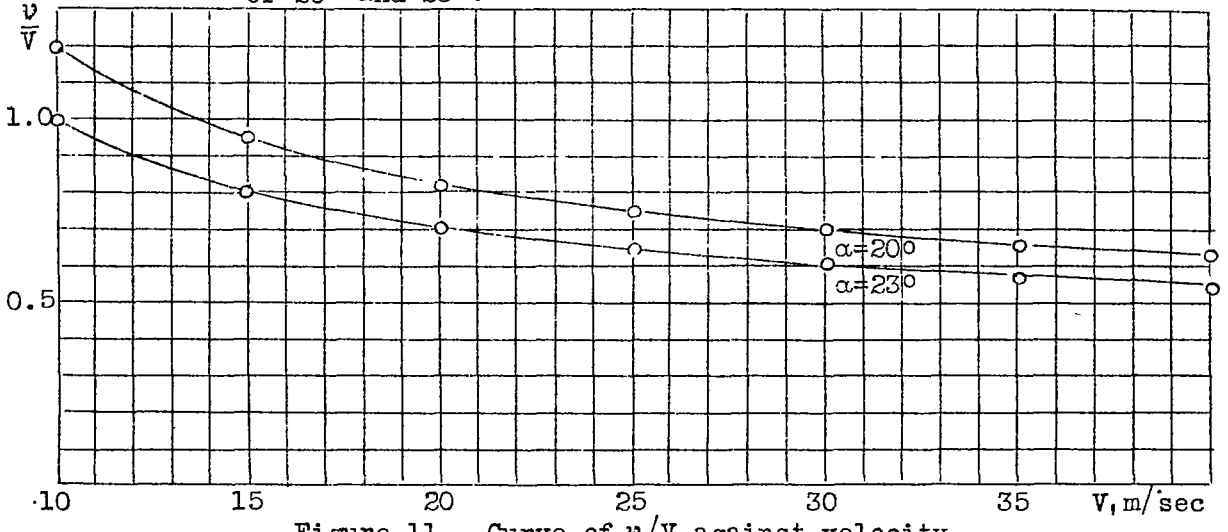

Figure 11.- Curve of ν/V against velocity.

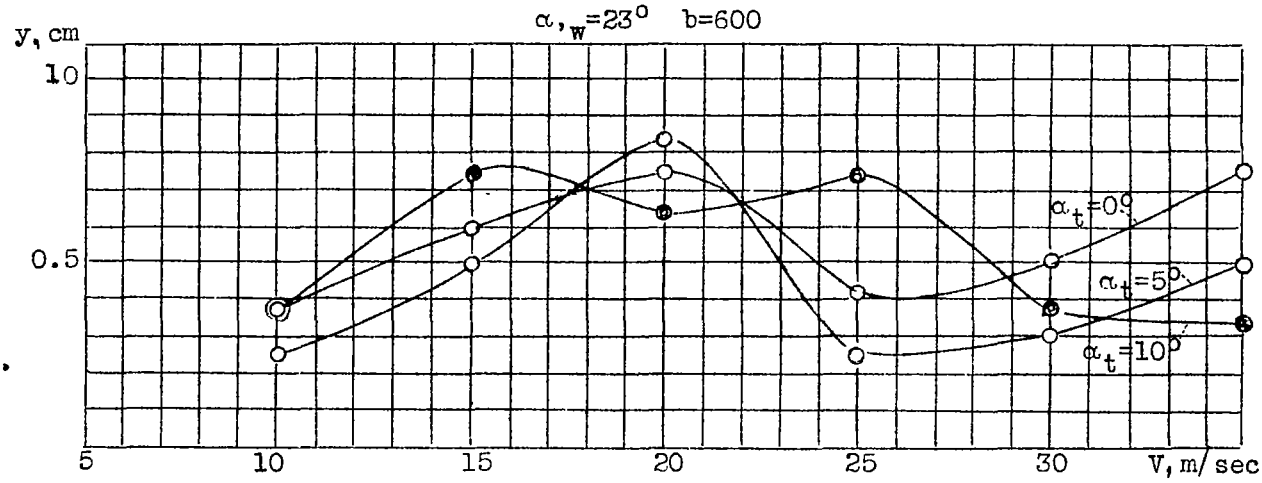

Figure 12.- Maximum deflections of tail surface for $\alpha_w=23^\circ$, $\alpha_t=5^\circ$ and 10°, wing chord 0.6 m.

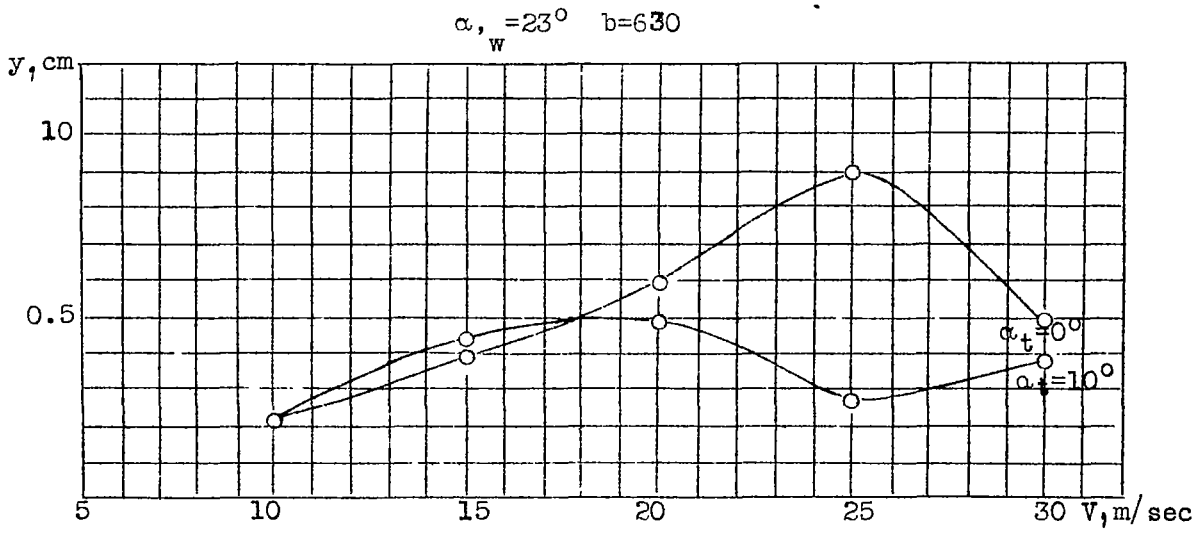

Figure 13.- Maximum deflections of tail surface for $\alpha_w=23^\circ$, $\alpha_t=0^\circ$ and 10°, wing chord 0.63 m.

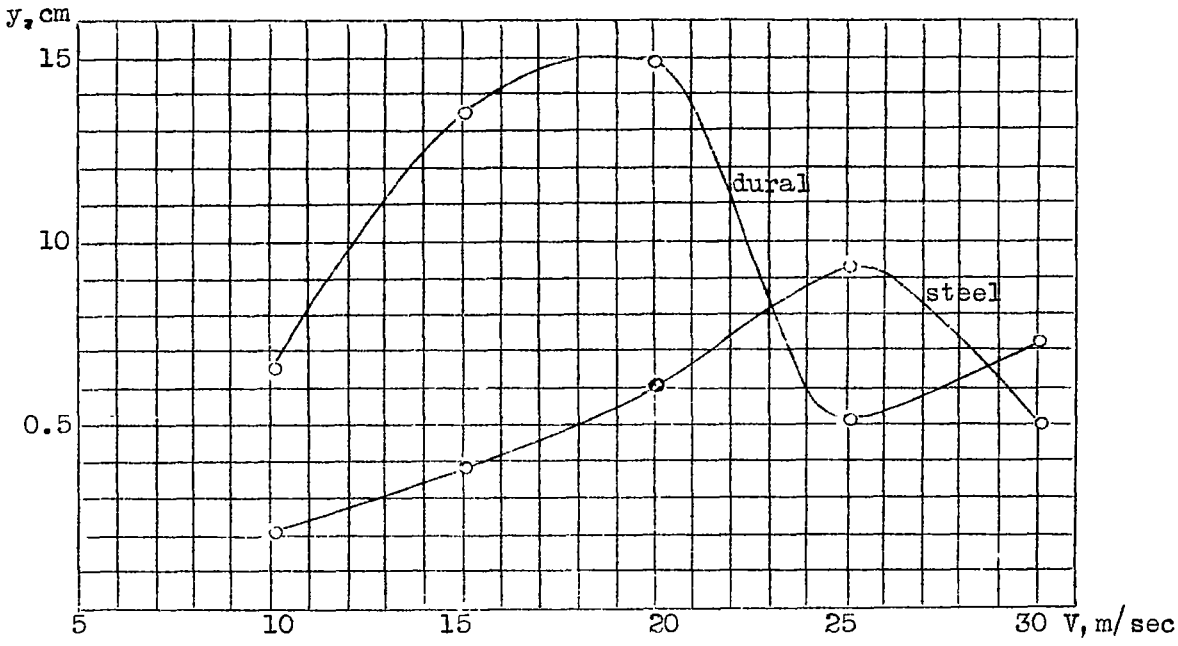

Figure 14.- Maximum amplitude of deflection of tips of tails of various stiffnesses.

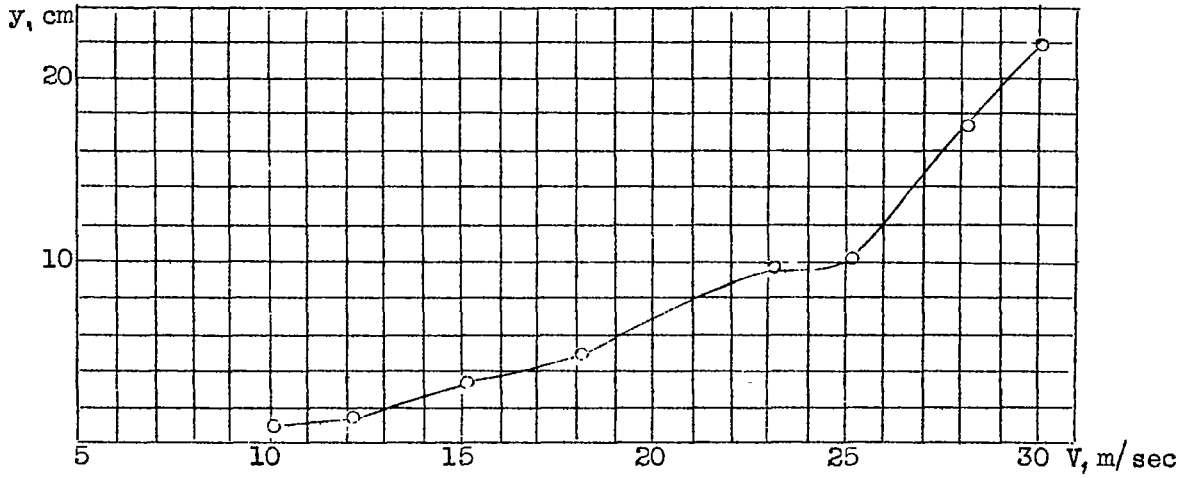

Figure 15.- Deflection of tip of tail for $\alpha_w=30^\circ$, wing chord 0.63 m, $\alpha_t=0^\circ$.

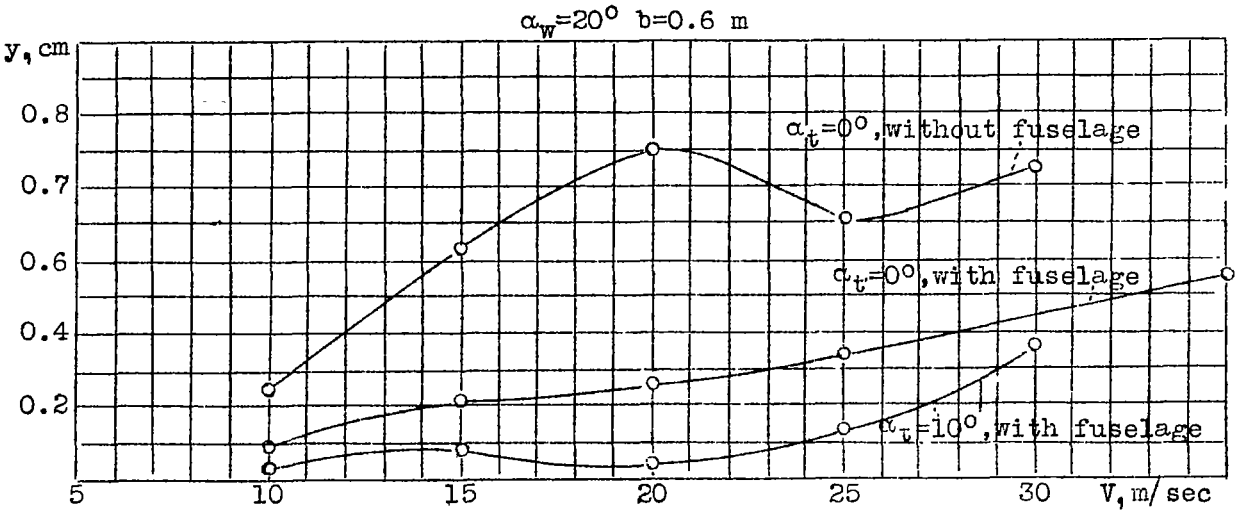

Figure 16.- Comparison curves of deflection of tip of tail for isolated wing and for combination of wing and fuselage.

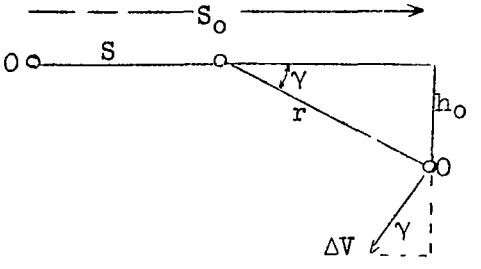

Figure 17.-

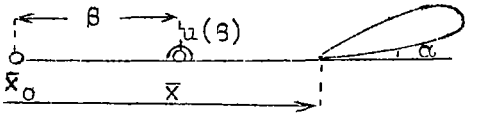

Figure 18.-

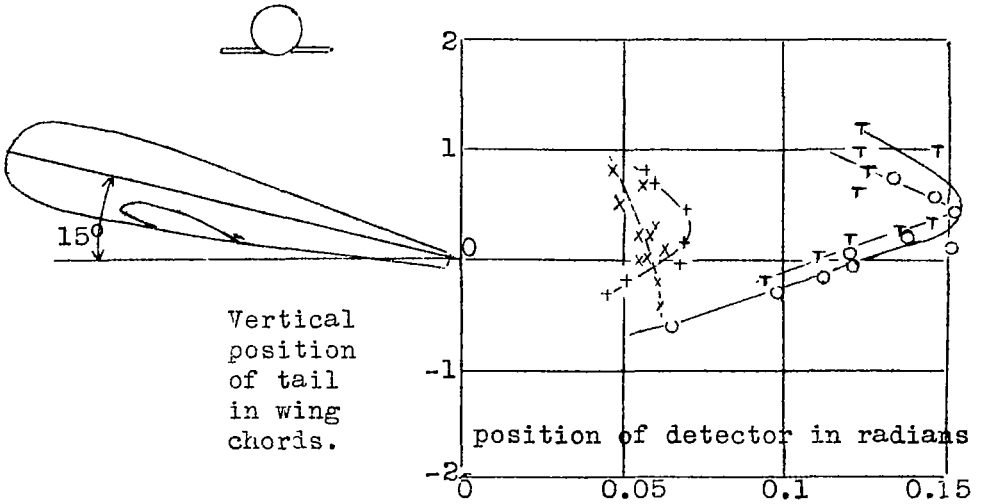

Figure 19.- Variation of maximum amplitude of deflection with vertical position of tail.

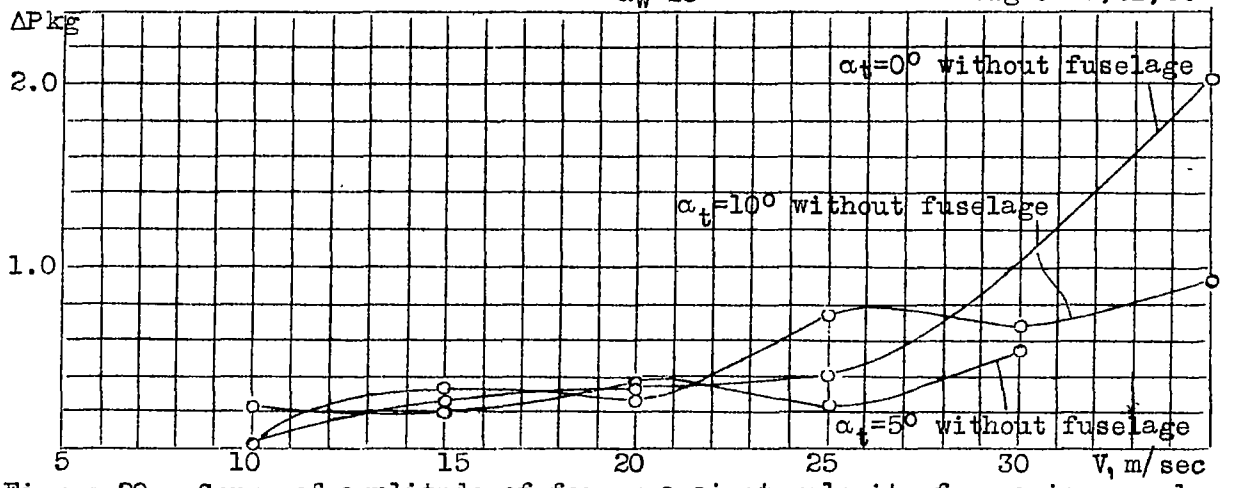

Figure 20.- Curve of amplitude of forces against velocity for various angles of attack of tail, wing angle of attack 23°.

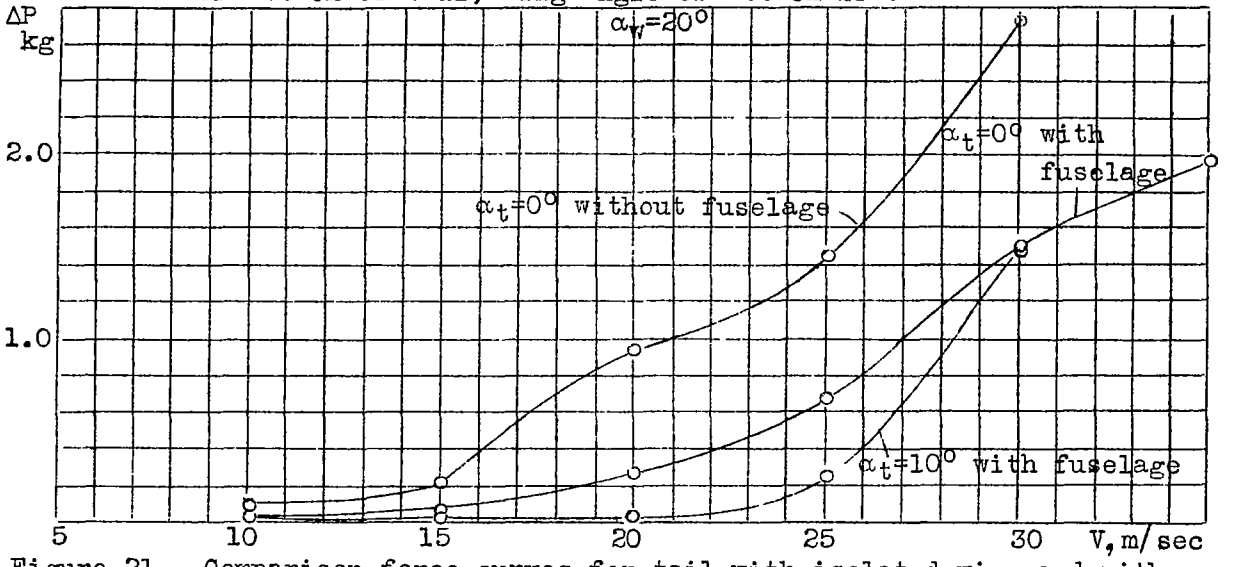

Figure 21.- Comparison force curves for tail with isolated wing and with combination of wing and fuselage.

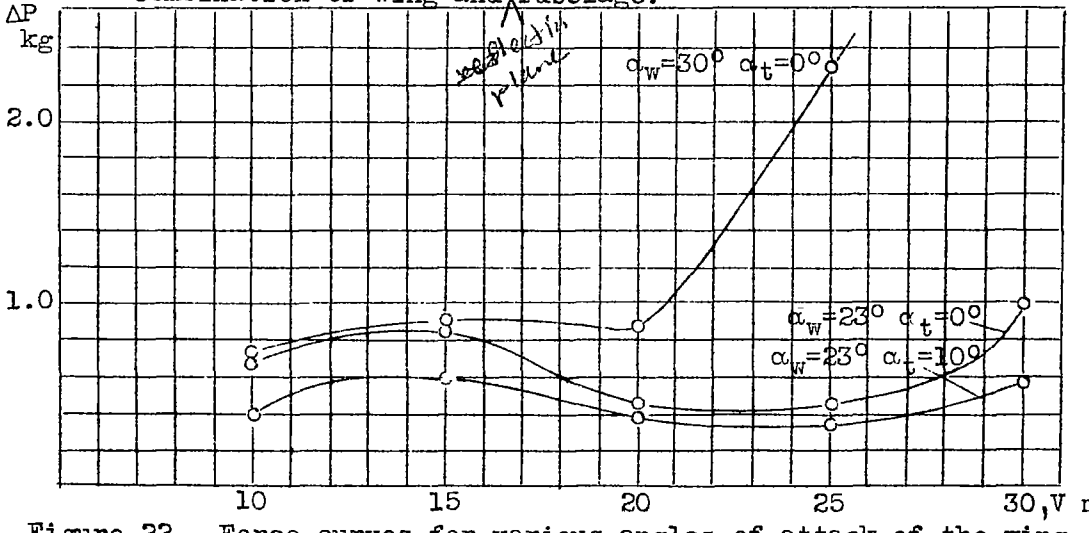

Figure 22.- Force curves for various angles of attack of the wing.

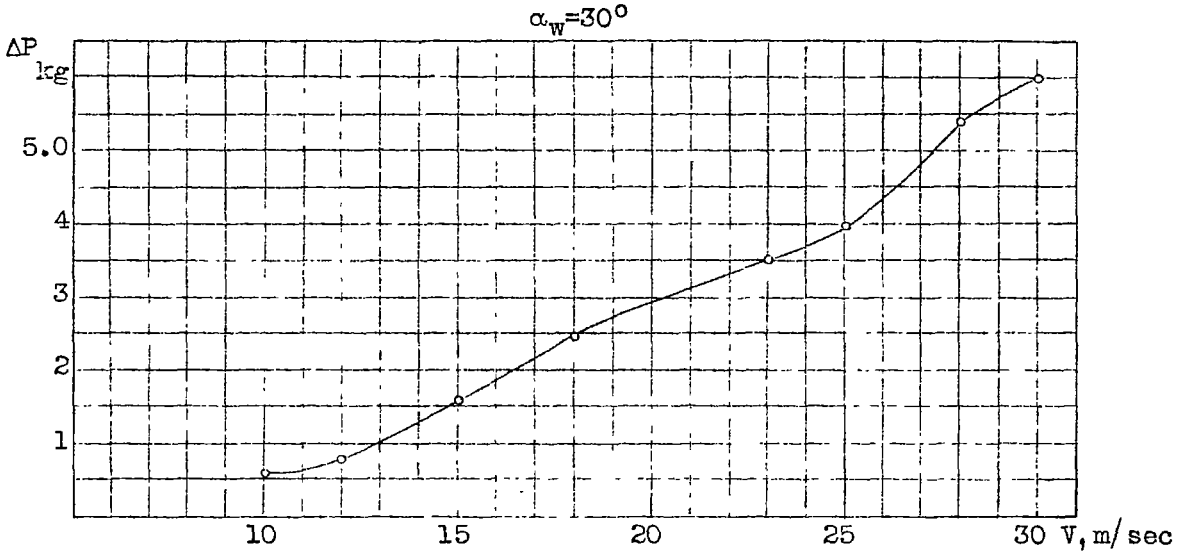

Figure 23.- Force curve for wing of chord 0.63 m. Angle of attack of tail 0°.

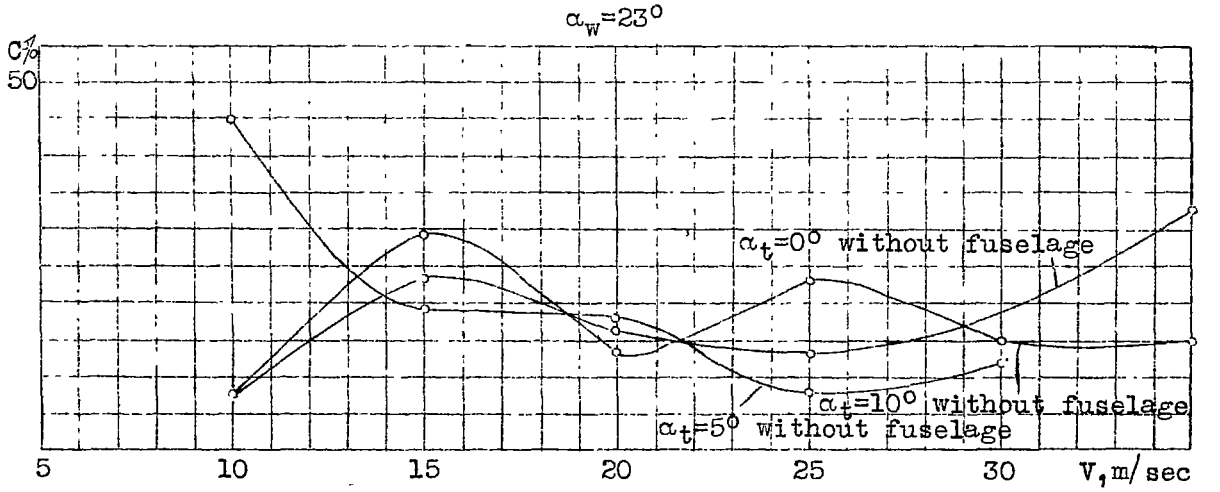

Figure 24.- Coefficient curves for various angles of attack of tail for wing angle of attack of 23°.

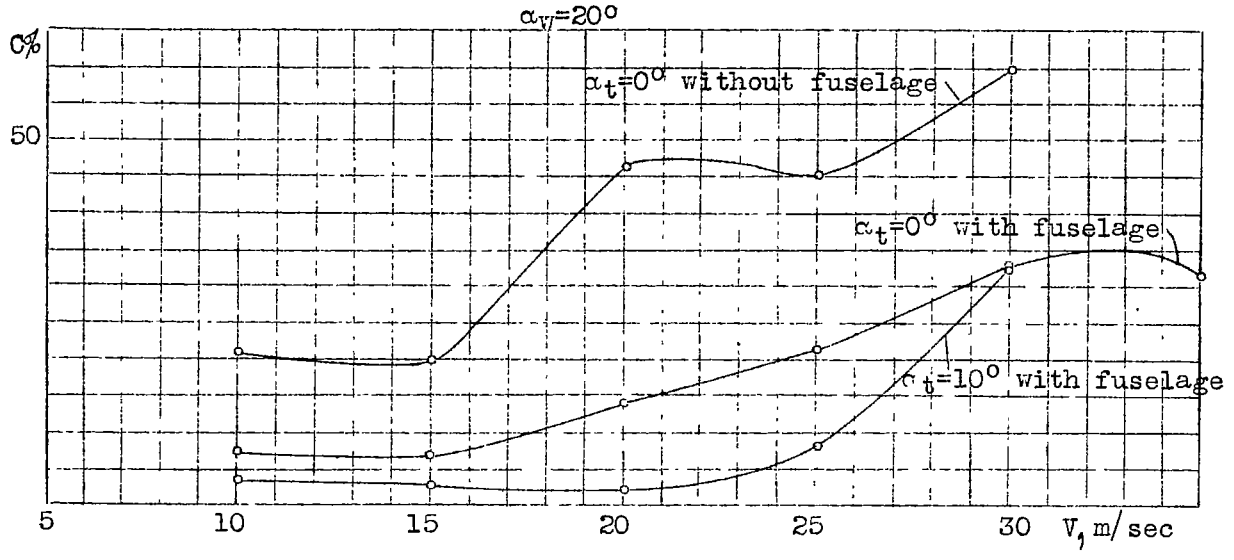

Figure 25.- Coefficient curves for isolated wing and combination of wing with fuselage.

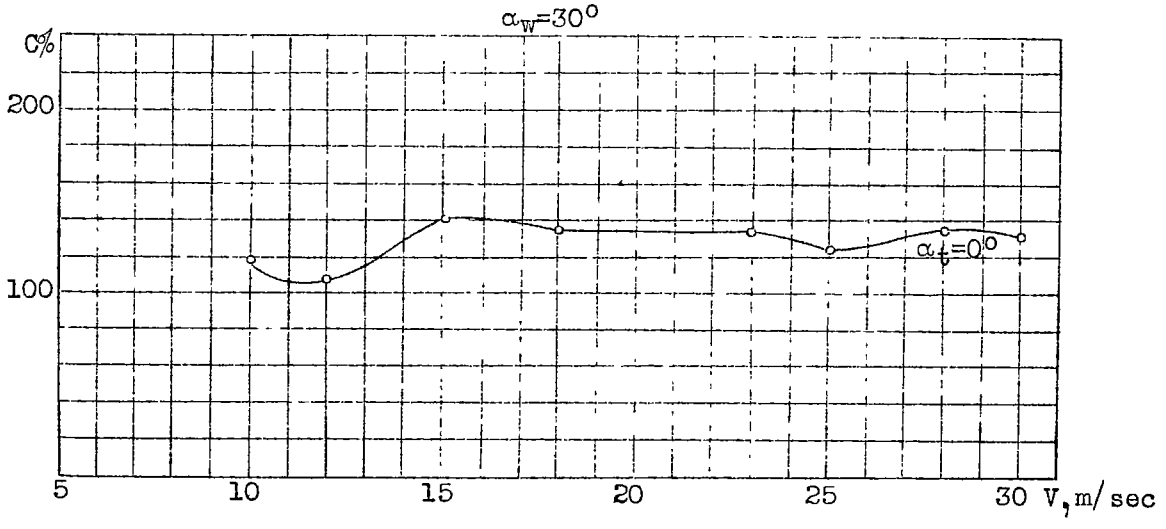

Figure 26.- Coefficient curve for wing angle of attack of 30°, chord 0.63 m.

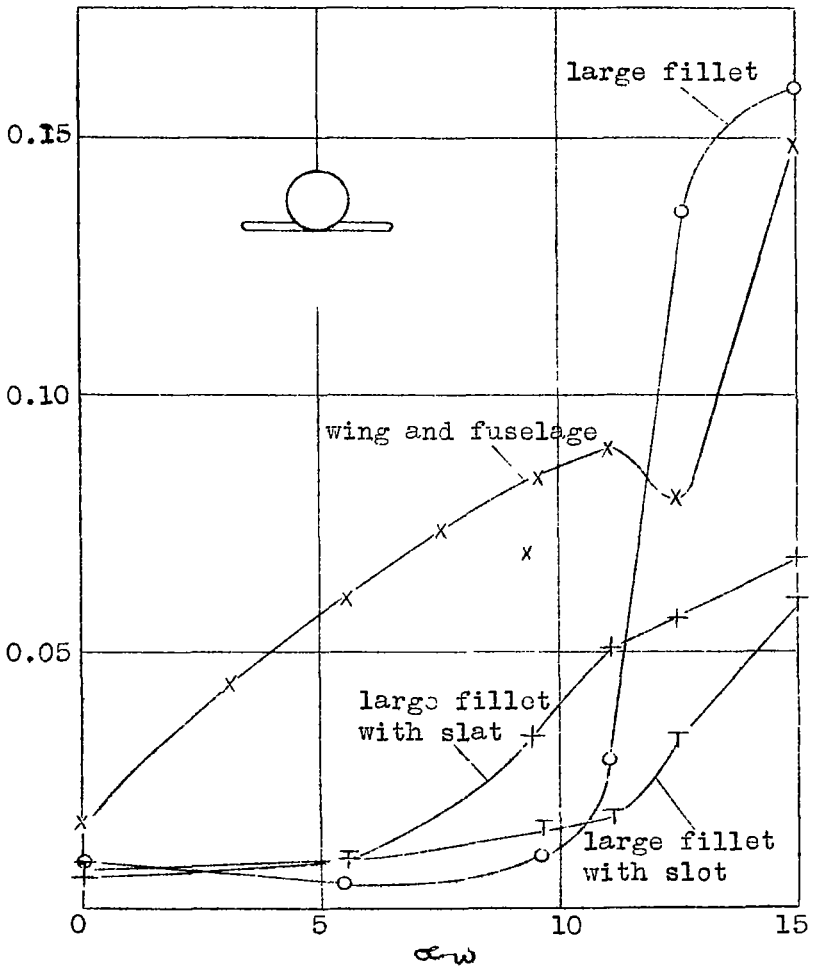

Figure 27.- Comparison of buffeting intensity for various devices to reduce buffeting. Ordinates give inclination of detector from mean position in radians, abscissas give angle of attack of wing.